NON-IONIC HIGHLY PERMEABLE POLYMER SHELLS FOR ENCAPSULATION OF LIVING CELLS

A Thesis
Presented to
The Academic Faculty

by

Jessica L. Carter

In Partial Fulfillment
of the Requirements for the Degree
Masters Degree in the
School of Materials Science and Engineering,
Bioengineering Program

Georgia Institute of Technology
May 2011

NON-IONIC HIGHLY PERMEABLE POLYMER SHELLS FOR ENCAPSULATION OF LIVING CELLS

Approved by:

Dr. Vladimir Tsukruk, Advisor
School of Materials Science and Engineering
Georgia Institute of Technology

Dr. Valeria Milam
School of Materials Science and Engineering
Georgia Institute of Technology

Dr. Meisha Shofner
School of Materials Science and Engineering
Georgia Institute of Technology

Date Approved: March 18, 2011

ACKNOWLEDGEMENTS

I would like to thank Irina Drachuk for her extensive assistance in data collection and analysis, and Drs. Veronika Kozlovskaya and Olga Shchepelina for helping with the direction of the project. I would also like to thank our Air Force Research Lab collaborators Dr. Svetlana Harbaugh and Dr. Nancy Kelley-Loughnane for hosting me for a summer, teaching me proper cell handling techniques, and providing project direction. This project is funded by the Air Force Office of Scientific Research FA9550-08-1-0446 and FA9550-09-1-0162 grants.

TABLE OF CONTENTS

LIST OF FIGURES

LIST OF SYMBOLS AND ABBREVIATIONS

D	Diffusion coefficient
PMBV	poly(2-methacryloyloxyethyl phosphorylcholine-co-n-butyl methacrylate-co-p-vinylphenylboronic acid
PVA	poly(vinyl alcohol)
PEG	poly(ethylene glycol)
PEG-NHS	*N*-hydoxysuccinimidyl-PEG
LbL	Layer-by-layer
PSS	poly(styrene sulfonate)
PAH	poly(allylamine hydrochloride)
PVPON	poly(N-vinylpyrrolidone)
TA	Tannic acid
PEI	poly(ethyleneimine)
CLSM	Confocal Laser Scanning Microscopy
FRAP	Fluorescence Recovery After Photobleaching
AFM	Atomic Force Microscopy
FITC	Fluorescein isothiocyanate
ROI	Region of Interest
yEGFP	Yeast enhanced green fluorescent protein
SMM	Synthetic minimal medium
RMS	Root mean square
OD600	Optical density at 600 nm
Gal	Galactose

SUMMARY

We introduce novel, *truly non-ionic* hydrogen-bonded layer-by-layer (LbL) coatings for cell surface engineering capable of long-term support of cell function. Utilizing the LbL technique imparts the ability to tailor membrane permeability, which is of particular importance for encapsulation of living cells as cell viability critically depends on the diffusion of nutrients through the artificial polymer membrane. Ultrathin, permeable polymer membranes are constructed on living cells without a cationic pre-layer, which is usually employed to increase the stability of LbL coatings. In the absence of the cytotoxic PEI pre-layer utilized in traditional LbL shells, viability of encapsulated cells drastically increases to 94%, as compared to 20-50% in electrostatically-bonded shells. Engineering surfaces of living cells with natural or synthetic compounds can mediate intercellular communication, render the cells less sensitive to environmental changes, and provide a protective barrier from hostile agents. Surface engineered cells show great potential for biomedical applications, including biomimetics, biosensing, enhancing biocompatibility of implantable materials, and may represent an important step toward construction of an artificial cell.

CHAPTER 1

INTRODUCTION

Benefits of Cell Encapsulation

Engineering surfaces of living cells with natural or synthetic compounds can mediate intercellular communication, render the cells less sensitive to environmental changes, and provide a protective barrier from hostile agents (Fig. 1).[1-4] The natural membrane, a selectively permeable phospholipid bilayer, is a good regulator of materials allowed in and out of the cell. However, for researchers to have control over this diffusion, an artificial environment is required.

Surface engineered cells show great potential for biomedical applications, including biomimetics, biosensing, enhancing biocompatibility of implantable materials, and may represent an important step toward construction of an artificial cell.[5,6]

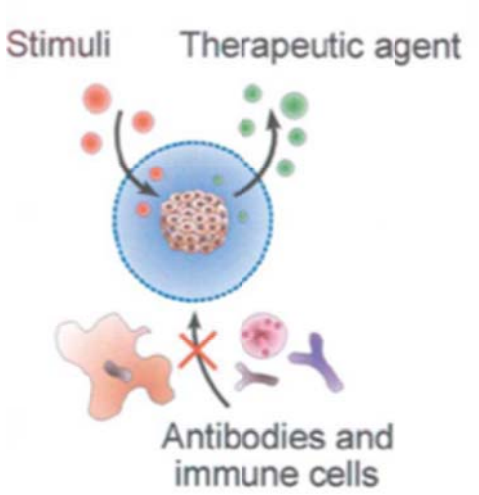

Figure 1: Cell encapsulation. Nutrients, oxygen, and stimuli diffuse across the membrane, whereas antibodies and immune cells are excluded.[4]

Motivations for engineering nanomaterials for cell encapsulation include protecting the cell through the use of semi-permeable membranes with *tunable* permeability while maintaining cell function by using materials which are non-toxic and do not limit the transport of nutrients. Cells enclosed in artificial membranes can be easily incorporated into artificial scaffolds used for engineering tissues or other parts of the body. Additionally, artificial membranes around cells can serve as a nurturing environment in which the encapsulated cells would essentially lie dormant until placed into appropriate "reviving" media with their function and viability restored.

Next, we will review methods of cell encapsulation, their benefits and drawbacks, and introduce our method and discuss its advantages.

Methods of Cell Encapsulation

Bulk Hydrogels

Hydrogels are a well-known and widely used method of cell encapsulation. They are of interest in biomaterials research because their watery structure provides a tissue-like environment for cells and promotes transport, enabling long-term survival of cells. The viscoelastic nature of hydrogels brings about some advantages: an injectable matrix can be implanted in the human body with minimal surgical wounds, and bioactive molecules or cells can be incorporated simply by mixing before injection.[7] A schematic of the typical hydrogel formation process is shown in Fig. 2. Thermosensitive hydrogels are especially attractive as specific injectable biomaterials due to their spontaneous gelation at physiological conditions, which does not require any extra chemical treatment.

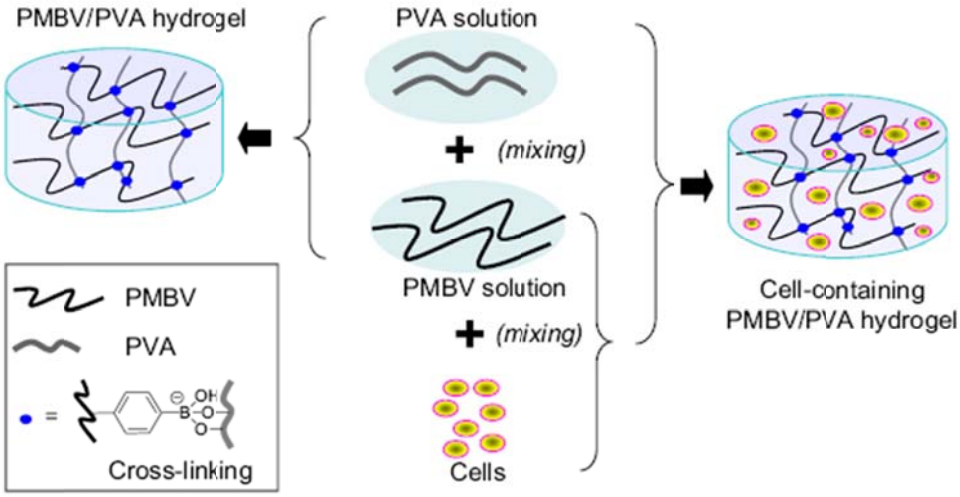

Figure 2: Schematic diagram of a typical hydrogel formation (poly(2-methacryloyloxyethyl phosphorylcholine-co-n-butyl methacrylate-co-p-vinylphenylboronic acid/polyvinyl alcohol) and fabrication of cell-containing hydrogel.[8]

Despite these benefits, hydrogels are also beset with a number of issues when used for cell encapsulation. To achieve desired mechanics, hydrogels are often crosslinked by high-energy irradiation, the application of addition and condensation reactions, and the use of aldehydes, all of which are incompatible with cell encapsulation.[9,10] Their innate nature as bulk materials result in slow diffusion through the hydrogel. These limitations seriously impede their practical and widespread use in cell-based assays.[8] Additionally, once the hydrogel network is formed, the structure and properties are fixed. This means that the solid biomaterial must be in its useful form (molecular weight, functionality, and architecture) upon conversion of the liquid precursors.[9]

Covalently Bonded Shells

Surface modification of living cells has also been achieved through covalent conjugation of polymers to amino groups of membrane proteins.[11,12,13] This method is

used because the wide variety of membrane proteins to which polymers can be covalently bonded means the method can be applied to many different cell types.[14] However, the strength and stability usually imparted by covalent bonding is not present here; coatings are not stable and polymers dissociate from the cell surface over time.[12,13] Additionally, the presence of these thick synthetic materials can adversely affect cell function by hindering the diffusion of nutrients.[14]

Shells via Hydrophobic Interactions with Amphiphilic Polymers

Cell surface modification using polyethylene glycol (PEG) and polyvinyl alcohol (PVA) conjugated amphiphilic polymers has been achieved by spontaneously anchoring the hydrophobic alkyl chains into the lipid bilayer of cell membranes.[11,14-16] This spontaneous anchoring can be achieved by simply incubating the amphiphilic polymers in the cell suspension. The hydrophobic chains will embed themselves into the cell membrane to escape the aqueous environment. Despite being incorporated into the cell membrane, amphiphilic polymers do not remain attached to the cell surface and dissociate into the surrounding medium.

Shells via Electrostatic Interactions

The innate negative charge on the cell surface is exploited in methods using electrostatic interactions. Cationic polymers interact with the cell surface, which is further modified using the layer-by-layer (LbL) technique.[11,17] Typically, a cationic pre-layer is deposited onto the cell surface. Next, anionic and cationic polymers are alternately adsorbed onto the surface until the desired number of bilayers (i.e. thickness) is achieved (Fig. 3).

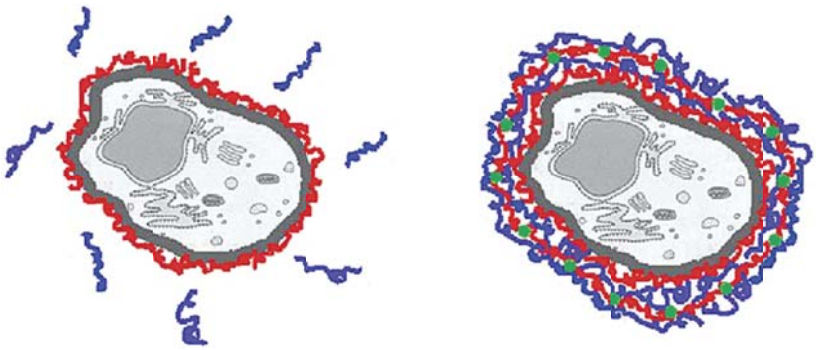

Figure 3: Vignette of the encapsulation process: consecutive adsorption of the polycation PAH (red) and the polyanion PSS (blue) onto a single living cell. To provide evidence of a successful coating, one or two layers are FITC-labeled PAH (green).[17]

Conformal coating of geometrically diverse templates, a precise control of the membrane thickness, and the ability to tune the membrane functionalities and properties are among the main advantages of the LbL approach.[18-25] The ability to tailor polymer membrane permeability is of particular importance for encapsulation of living cells, as cell viability critically depends on the diffusion of nutrients through the artificial polymer membrane.

Despite examples of successful applications of the LbL assembly for encapsulation of living cells (Fig. 4), cytotoxicity of the polycations used in conventional LbL assembly—poly(styrene sulfonate) (PSS) and poly(allylamine hydrochloride) (PAH)—pose severe limitations on the potential application of the LbL approach to cell surface engineering.[26,27] It has been suggested that overall toxicity of the polyelectrolytes originates from the positive charge of polycations. This charge results in pore formation within the cell membrane, causing its damage and, eventually, cell death.[28-32]

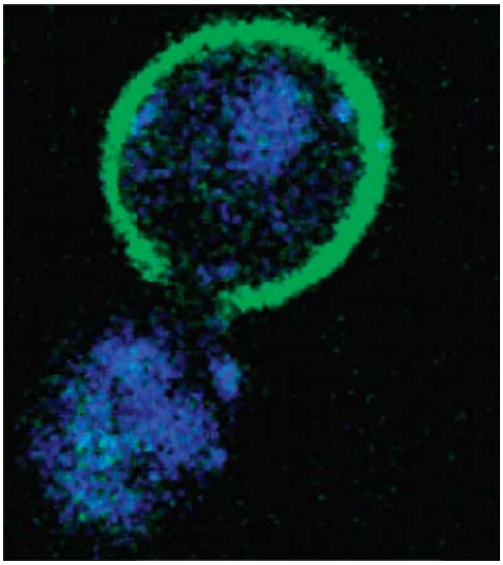

Figure 4: Yeast cells coated with PAH/PSS for immunoprotection.[18]

Hydrogen-Bonded Shells

In contrast to traditional ionically paired polyelectrolyte LbL multilayers, hydrogen bonded shells facilitate gentle encapsulation using non-toxic, non-ionic, and biocompatible components.[31] Hydrogen-bonded LbL assembly also facilitates facile production of films responsive to environmental pH and/or temperature at mild pH values.[32] Thus, the hydrogen-bonded LbL assembly of films and shells allows for incorporation of uncharged biocompatible functional polymers, such as poly(N-vinylpyrrolidone) (PVPON).[33,34]

Research in this area by Kozlovskaya et al. began with LbL construction of hollow multilayer shells on silica microparticles used as sacrificial templates.[33] A schematic of this process is shown in Fig. 5a. Hydrogen-bonded (tannic acid/non-ionic polymer) coatings can be formed either through deposition on poly(ethyleneimine) (PEI)-treated silica particles (1A) starting from tannic acid (TA) or through direct deposition of

the (non-ionic polymer/TA) multilayer starting from a neutral polymer (1B). When a desired number of the bilayers is achieved (2), silica cores are etched out leaving behind hollow capsules (3).

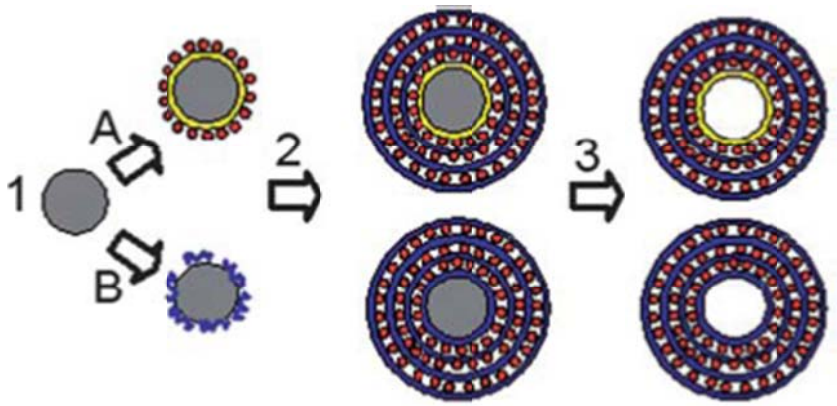

Figure 5: General schematic of the LbL (TA/non-ionic polymer) capsule formation based on hydrogen bonding.[33]

Shell thickness and permeability could be controlled by changing the molecular weight of the shell components, a simpler method than is necessary in ionically assembled LbL shells, where deposition conditions, e.g., pH or ionic strength, must be changed to achieve a similar effect.[33] In Fig. 6 we see a confocal laser scanning microscopy (CLSM) image of PEI(TA/PVPON)$_3$ capsules in aqueous solution, with an inset of bare silica microparticle templates.

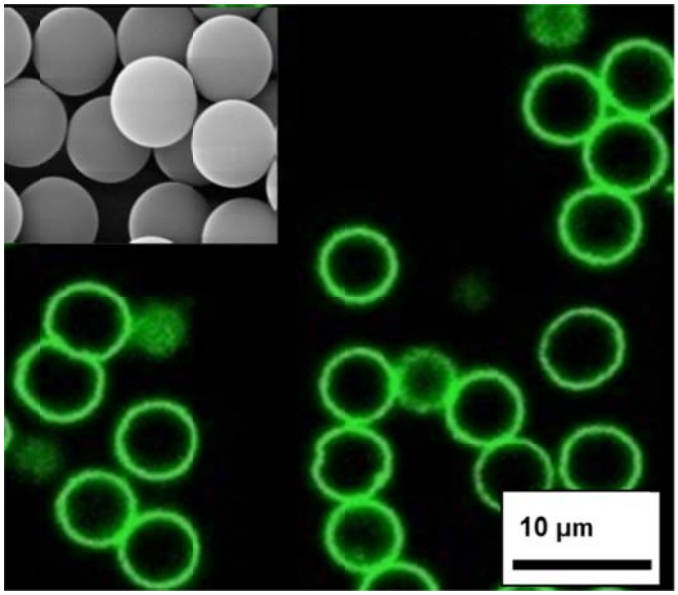

Figure 6: CLSM image of hollow PEI(TA/PVPON)$_3$ capsules in aqueous solution. Inset: bare silica microparticle templates.[35]

In order to design individual *cell-compatible* synthetic shells, we recently designed highly permeable, hydrogen-bonded LbL coatings utilizing a pre-layer poly(ethyleneimine) (PEI) along with TA and PVPON, which result in nanocoatings responsive under biologically and physiologically relevant conditions that are suitable for engineering cell surfaces while increasing cell viability.[31-38] Fig. 7 shows TEM images of freeze-dried bare (7a) and cells coated in PEI(TA/PVPON) (7b). In Fig. 7c, a CLSM image of PEI(TA/PVPON)-coated cells is seen, where the outer layer of PVPON is labeled with Alexa Fluor 532, whose red fluorescence provides visual conformation of the polymer membranes.

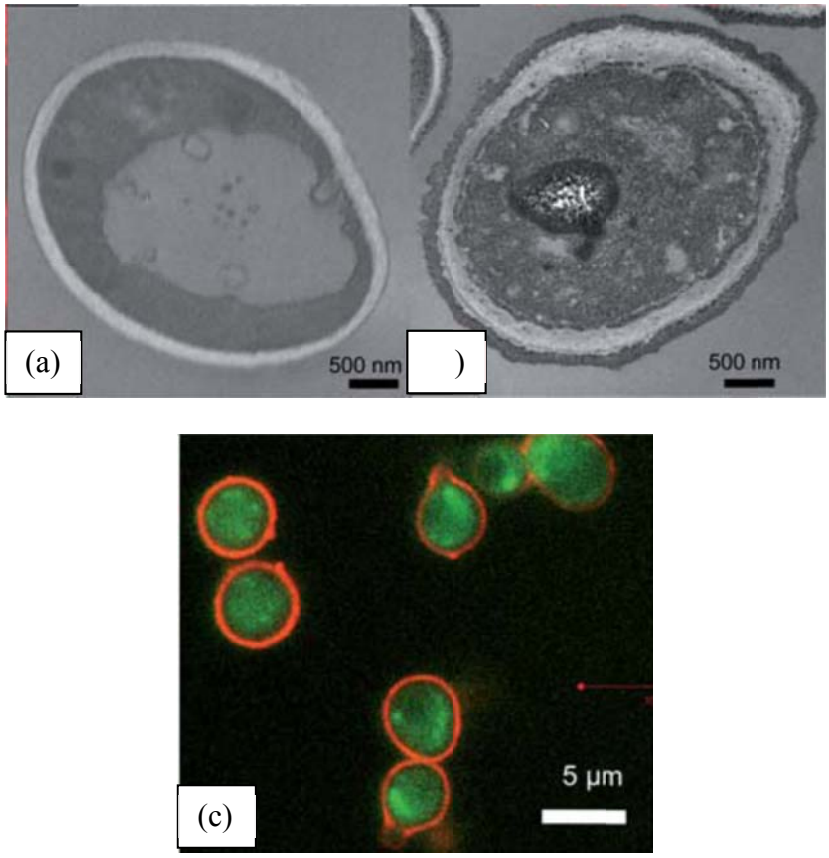

Figure 7: TEM images of freeze-dried (a) bare and (b) PEI(TA/PVPON) coated YPH501 yeast cells. (c) CLSM image of PEI(TA/PVPON)$_3$-coated cells with Alexa Fluor 532-PVPON-labelled outer layers.[31]

In these PEI(TA/PVPON) systems, cell viability following encapsulation was increased to 79%, as opposed to merely 20% in conventional PSS/PAH systems. This was attributed to increased diffusion through the hydrogen-bonded shells.

In the application of the LbL technique to cell surfaces, the use of a precursor layer such as PEI can provide several advantages. First, because cell surfaces are negatively charged, deposition of a PEI layer reverses the surface charge and can provide enhanced adhesion of the subsequent mutilayers. In addition, PEI is known to strongly adsorb onto a majority of surfaces regardless of their charge, likely due to strong non-

electrostatic contributions to the adsorption energy.[39-41] This allows the use of PEI as an almost universal priming layer that eliminates many of the uncertainties associated with a poorly defined surface charge. However, the cytotoxicity of PEI has a negative effect on cell function.[42] Consequently, an encapsulation method that would increase cell viability without sacrificing the desired diffusion properties and mechanical stability of the shells achieved previously would be valuable.

Therefore, we introduce novel, *truly non-ionic* hydrogen-bonded LbL coatings for cell surface engineering capable of long-term support of cell function. In this study, we show that ultrathin, permeable polymer membranes can be constructed on living cells without a cationic pre-layer. In the absence of the cytotoxic PEI pre-layer, viability of encapsulated cells climbs to 94%. The membranes display vastly improved diffusion properties and their mechanical properties allow cells to grow and divide through membrane rupture.

Electrostatic vs. PEI Hydrogen-Bonded Shell Performance

Cell Viability

To show that the presence of ionic components was responsible for LbL shell cytotoxicity, comparative studies were conducted between hydrogen-bonded and ionic LbL shells.[31] Unlike the PAH/PSS shells, hydrogen-bonded shells exerted much lower, 5%, cytotoxicity with subsequent bilayers assembled. The initial decrease in cell viability in the case of PEI(TA/PVPON) shells can be attributed to the PEI pre-layer. Assembly of 3- and 4-bilayer PEI(TA/PVPON) LbL shells maintained high viability up to 79% in contrast to polyelectrolyte (PAH/PSS) shells, which caused up to 88% cell death (Fig. 8).

These results were consistent with the PAH/PSS cytotoxicity vastly reported in literature.[11]

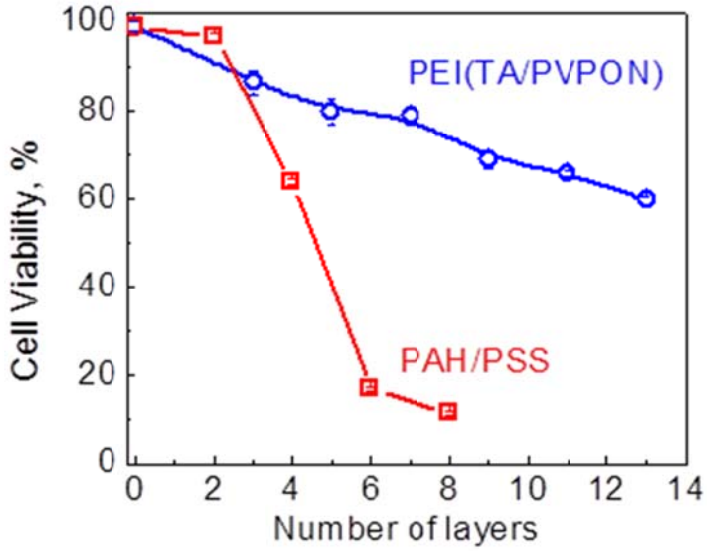

Figure 8: Comparison of cell viability (%) for (PAH/PSS) and PEI(TA/PVPON) coatings tested with resazurin assay.[31]

Shell Thickness

Fluorescence Recovery After Photobleaching (FRAP) experiments are used to model the permeability of nutrients through the shells. Permeability through hydrogen-bonded shells was shown to be dramatically higher for comparable number of PAH/PSS bilayers with diffusion coefficient reaching $D = 8 \times 10^{-12}$ cm^2 s^{-1}, which is almost five times higher than that known for traditional polyelectrolyte LbL shells.[31] The observed difference for diffusion coefficients between PAH/PSS and PEI(TA/PVPON) shells can be attributed to loose, grainy morphology of the PEI(TA/PVPON) LbL multilayers (Fig. 9) characteristic of hydrogen-bonded systems. The highly permeable structure of hydrogen-bound shells is critical for the transport of nutrients towards coated cells.

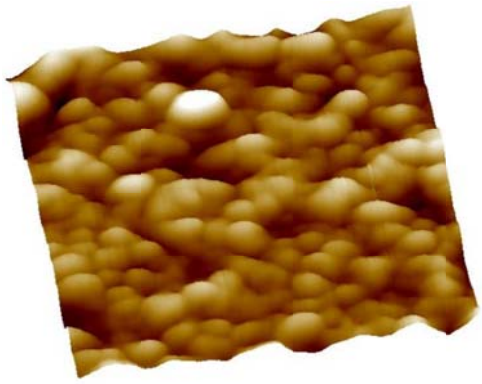

Figure 9: 3D topographical AFM image of PEI(TA/PVPON)$_4$ hollow shells dried on a silicon wafer. Scale is 500 nm x 500 nm x 50 nm.[31]

CHAPTER 2

GOALS & OBJECTIVES

The goal of the study is to develop truly non-ionic hydrogen-bonded polymer shells in order to increase the viability of encapsulated cells. Though hydrogen-bonded shells which utilize a cationic pre-layer are stable and result in better cell viability than other methods of encapsulation, these pre-layers, specifically PEI, are cytotoxic to cells. Therefore, we expect construction of these shells in the absence of a cationic pre-layer will increase cell viability.

We will address whether hydrogen-bonded shells can, in fact, be constructed in the absence of a pre-layer, and whether this can be done without compromising shell stability. Additionally, we will explore whether these truly non-ionic hydrogen-bonded shells show greatly improved cell viability, and why or why not this effect is seen. We believe changes in cell viability may be related to the rate of diffusion through the shells and the thickness of the shells.

In developing these polymer shells, we seek to characterize their morphology, including surface topography, effect on cell viability, and the ability of small molecules to diffuse through the shell.

This study will facilitate understanding the fundamentals of interfacial organization and interactions of responsive synthetic macromolecular nanomaterials at the cell surface for intelligent cell surface engineering.

CHAPTER 3

METHODS

Layer-by-layer (LbL) Assembly

The LbL assembly was employed for encapsulation of individual yeast cells with hydrogen-bonded multilayers of TA/PVPON.[35,37] This process is illustrated in Fig. 10. Before deposition of (TA/PVPON) multilayer membranes, yeast cells were harvested in 1.5 mL centrifuge tubes by centrifugation at 2000 rpm for 4 minutes and washed three times in phosphate buffer (0.01 M in 0.1 M NaCl, pH = 6). LbL deposition of hydrogen-bonded TA/PVPON layers from solutions of the same concentrations dissolved in 0.01 M phosphate buffer and 0.1 M NaCl at pH = 6. During LbL deposition, cells were re-dispersed in the appropriate solution by gentle shaking (at 225 rpm) for 15 minutes. After deposition of each layer, cells were collected in a pellet by centrifugation and washed three times with phosphate buffer.

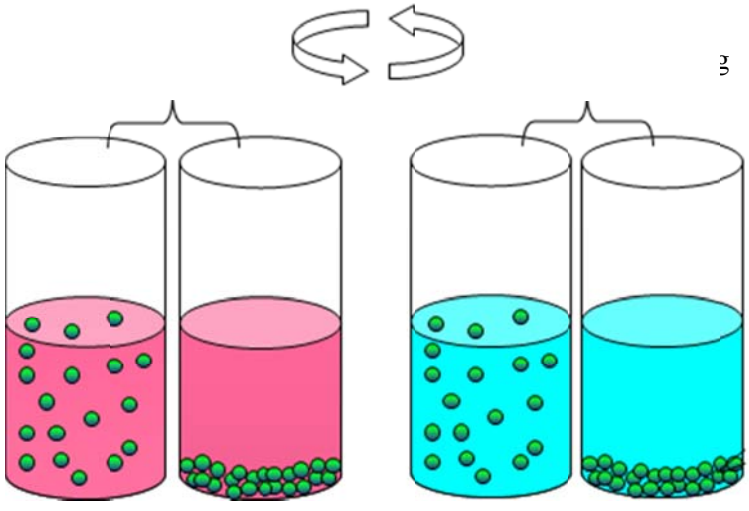

Figure 10: Schematic illustrating LbL assembly of hydrogen-bonded layers.[33]

All solutions were filter-sterilized with polystyrene nonpyrogenic membrane systems (0.22 mm pore size) (Corning filter system) before applying to the cells. When hollow shells of (TA/PVPON) were needed for diffusion experiments, the hydrogen-bonded multilayers were assembled onto silica particles in the same manner described above.[35]

Atomic Force Microscopy (AFM)

AFM was used to study the morphology of coated cell surfaces. We perform these measurements to visualize the initial roughness (signifying polymer adhesion) and subsequent smoothing of cell surfaces (signifying uniform coverage). AFM images were collected using a Dimension-3000 (Digital Instruments) microscope in the "light" tapping mode according to the well-established procedure.[43]

ζ-potential

Independent measurements of ζ-potentials on encapsulated yeast cells after deposition of each layer were performed on Zetasizer Nano-ZS equipment (Malvern). Yeast cells were collected at mid-log phase (OD = 0.6–0.8), washed three times in a solution of 0.01 M phosphate buffer and 0.1 M NaCl at pH 6.0 before depositing subsequent layers of TA and PVPON (Mw = 360 kDa). After deposition and washing, 100 mL of encapsulated cells were combined with 900 mL of deionized Nanopure water to obtain 1 mL of solution to perform ζ-potential measurements. Each value was acquired by averaging three independent measurements of 40 sub-runs each.

Confocal Laser Scanning Microscopy (CLSM)

Confocal images of encapsulated and non-encapsulated yeast cells were obtained with an LSM 510 NLO META inverted confocal microscope equipped with 63 x 1.4 oil

immersion objective lens (Zeiss, Germany). Before imaging, cells were washed three times in deionized water to reduce background auto-fluorescence from the SMM medium. Coated or uncoated yeast cells were seeded in Lab-Tek chamber glasses (Electron Microscopy Sciences) for half an hour before imaging. The 488 nm excitation from the Argon ion laser and 514 nm emission wavelengths were used for yEGFP visualization, whereas 543 nm excitation (He–Ne laser) and 565 nm emission were used to visualize fluorescently labeled polymer shells surrounding yeast cells.

Resazurin Assay

Cell viability was measured using resazurin assay. Control (non-treated) and encapsulated cells were re-suspended in 1 mL of media. 100 mL of resazurin (7-hydroxy-3H-phenoxazin-3-one 10-oxide) solution was added to cell cultures. The mixtures were incubated at 30 ºC for 2 hours. Fluorescence was measured at $\lambda = 590$ nm ($\lambda_{Ex} = 560$ nm).

Fluorescence Recovery After Photobleaching (FRAP)

Experiments on permeability were performed using CLSM[44] and the fluorescence recovery after photobleaching (FRAP) method. The basic principle of FRAP is illustrated in Fig. 11. Hollow capsules of hydrogen-bonded TA/PVPON with 4, 5 and 6 bilayers were prepared as described elsewhere.[33] 100 mL of hollow capsules solution was combined with 200 mL of 1 mg mL^{-1} fluorescein isothiocyanate (FITC) solution (pH = 6) and allowed to settle down in a Lab-Tek chamber glass cell for three hours. Laser beam (488 nm) was focused within a region of interest (ROI) inside a capsule, and pulsed at 100% intensity to photobleach the dye molecules.

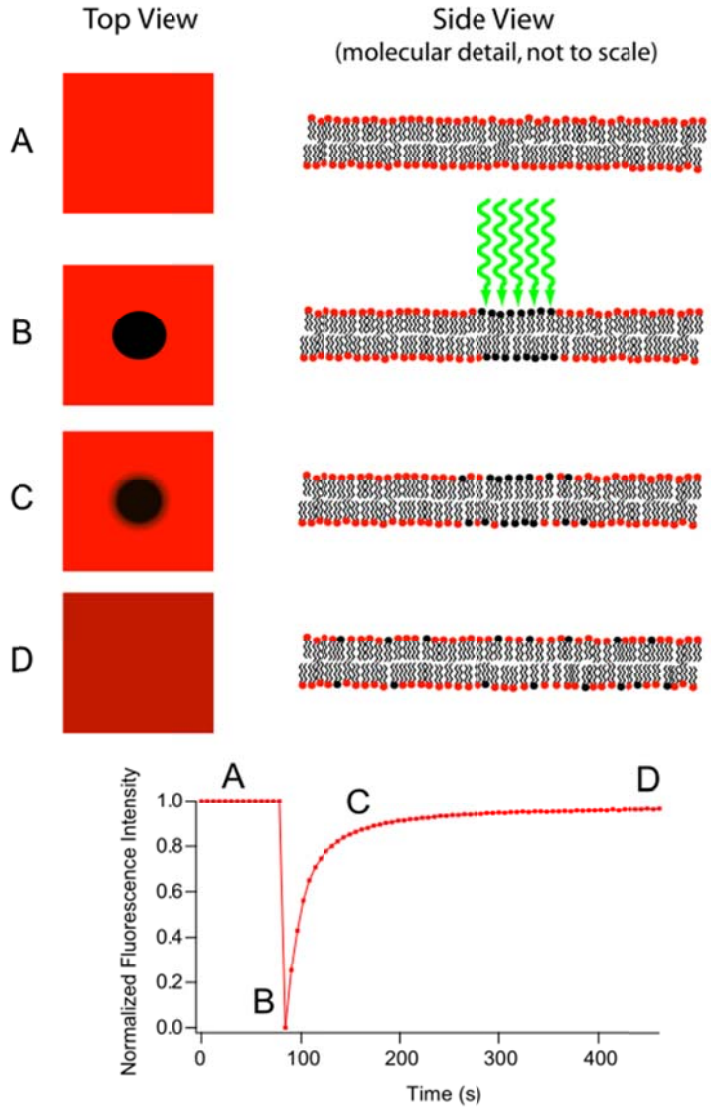

Figure 11: Principle of FRAP A) The bilayer is uniformly labeled with a fluorescent tag B) This label is selectively photobleached by a small fast light pulse C) The intensity within this bleached area is monitored as the bleached dye diffuses out and new dye diffuses in D) Eventually uniform intensity is restored.[45]

Each experiment started with 3 prebleached image scans followed by 25–35 bleach pulse exposures of 3 ms each within ROI. The bleaching time was adjusted to ensure complete photobleaching of FITC inside the capsule. The fluorescence recovery was monitored by capturing 30 scans of 3 ms exposure at 3% laser intensity. The

recovery was considered complete when the intensity of the photobleached region stabilized. The quantitative analysis was performed using ImageJ software, and curve-fitting was conducted in Origin. The recovery curve of the fluorescence intensity, I(t), as a function of time, t, was fit by:

$$I = I_0(1 - e^{-At}) \quad (1)$$

where I and I_0 are the equilibrium and initial fluorescence intensities, respectively. The coefficient A is related to the diffusion coefficient, D, according to:

$$A = 3D/rh \quad (2)$$

for FITC diffusion through a spherical wall with radius r and thickness h. In the solution, eqn (1) obeys Fick's law and can be written as:

$$dc/dt = -A(c - c_0) \quad (3)$$

where c and c_0 are the concentrations inside and outside the capsules, respectively, and $c \approx I$. A typical fit of the recovery curve was obtained using eqn (1) and the coefficient A was deduced from the fitting.[46-48]

CHAPTER 4

RESULTS & DISCUSSION

Morphology of LbL Shells

LbL shells of sequentially applied $(TA/PVPON)_n$ were formed around the YPH501 cells. Hydrogen bonding between the hydroxyl groups of TA and the carbonyl groups of PVPON preserve cell integrity and functioning under deposition conditions.[49-33] Fig. 12 illustrates the LbL assembly of hydrogen-bonded shells around living cells.

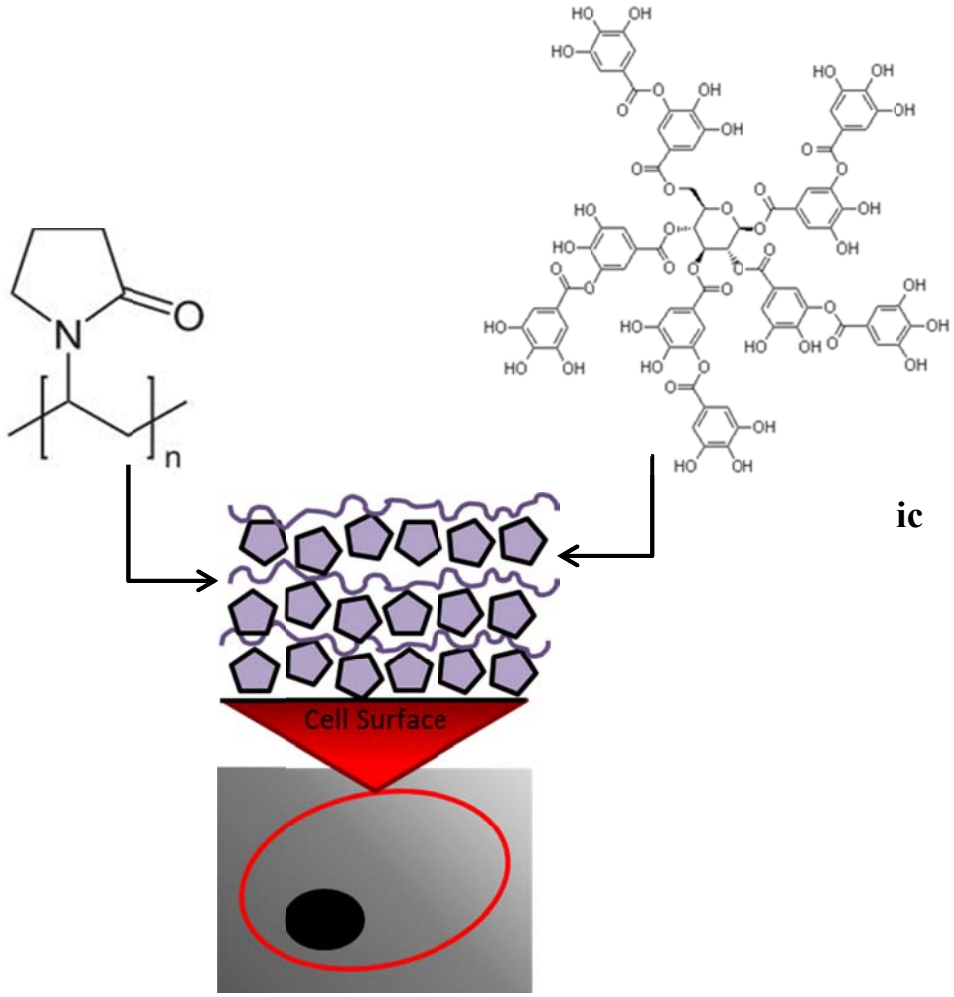

Figure 12: Schematic illustrating formation of hydrogen-bonded TA/PVPON shell layer-by-layer on yeast cell surfaces and LbL assembly of hydrogen-bonded layers

Materials

Tannic acid (TA) (Mw = 1700 Da), poly(N-vinylpyrrolidone) (Mw = 360 000 Da and Mw = 1 300 000 Da) (PVPON), mono- and dibasic sodium phosphate, galactose, and glucose were purchased from Sigma-Aldrich. Alexa Fluor 532 carboxylic acid succinimidyl ester fluorescent dye was purchased from Invitrogen. Ultrapure (Nanopure system) filtered water with a resistivity of 18.2 MΩ cm was used for experiments.

The *S. cerevisiae* YPH501 diploid yeast strains expressing yEGFP (yeast enhanced green fluorescence protein) were used for this study. Cells were cultured in synthetic minimal medium (SMM) supplemented with appropriate dropout solution and sugar source, 2% glucose. Yeast cells were grown at 30 ºC in a shaker incubator (New Brunswick Scientific) with 225 rpm to bring them to an early exponential phase.[52]

Evaluation

Polymer shells were constructed around *S. cerevisiae* cells using LbL, as described in the methods section. Hydrogen bonding between the hydroxyl groups of TA and the carbonyl groups of PVPON preserve cell integrity and functioning under deposition conditions.[33,49,50,51] The successful formation of shells around cells was confirmed by confocal microscopy. Alexa Fluor 532-labeled PVPON was used to validate the presence of polymer shells. Homogeneous fluorescence from Alexa Fluor 532-fluorescently tagged PVPON, which confirms formation of the polymer membrane, is shown in Fig. 13.

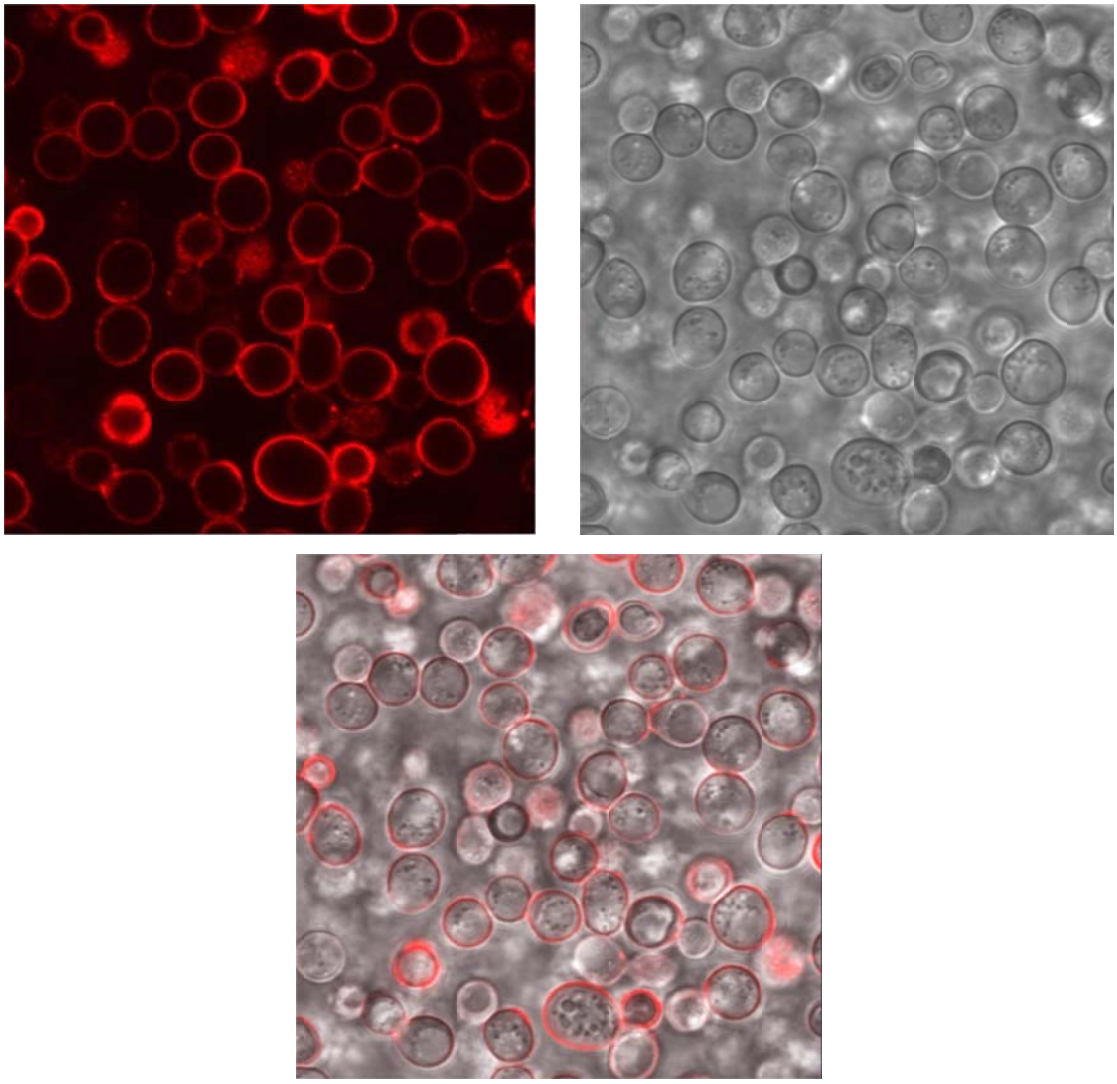

Figure 13: CLSM images of $(TA/PVPON)_4$ coated cells. (a) Large scale confocal image of encapsulated yeast cells with fluorescently labeled PVPON-co-Alexa Fluor 532. (b) The same area in transmitted mode. (c) Overlapped images from both fluorescent and transmitted modes.

Fig. 13a demonstrates large scale confocal image of encapsulated yeast cells with fluorescently labeled PVPON-co-Alexa Fluor 532. Fig. 13b shows the same area in

transmitted mode. By overlapping images from both florescent and transmitted modes (Fig. 13c), one can confirm that all the cells visible in the selected area have been coated.

We perform AFM measurements to visualize the surface morphology of coated cell surfaces and evaluate the initial microroughness and subsequent smoothing of cell surfaces. AFM topographical images show overall shape and dimensions of cells as well as fine surface features for (a) bare, single bilayer with polymer concentrations of (b) 0.5 mg/mL and (d) 2 mg/mL, and two bilayers with concentrations of (c) 0.5 mg/mL and (e) 2 mg/mL. Average root mean square (RMS) roughness was taken from a 100nm square measurement area on 2 μm AFM scans.

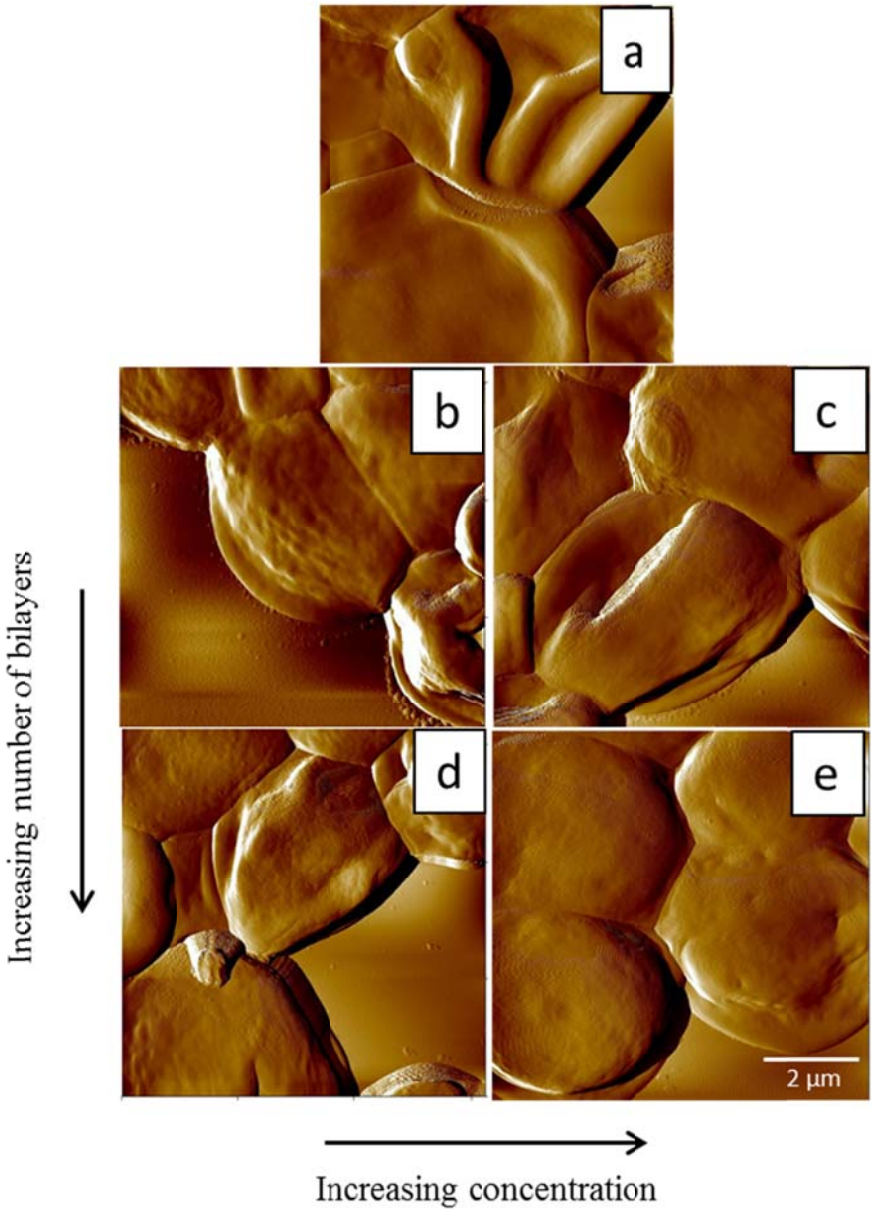

Figure 14: AFM amplitude images of (a) bare and (b)-(e) coated YPH501 yeast cells. (b) 1 bilayer, 0.5 mg/mL; (c) 1 bilayer, 2 mg/mL; (d) 2 bilayers, 0.5 mg/mL; (e) 2 bilayers, 2 mg/mL

Figs. 14a and 14b show that deposition of (TA/PVPON) significantly increased the roughness of uncoated cells, from 3.87 ± 2.23 nm to 9.33 ± 2.92 nm. AFM measurements also show that roughness decreases slightly with an increase in

TA/PVPON bilayers (Fig. 14c and 14e) by approximately 22% (from 4.64 ± 2.74 nm to 3.47 ± 1.32 nm), and decreases significantly with an increase in polymer concentration (Fig. 14d and 14e) by approximately 52% (from 7.59 ± 2.84 nm to 3.47 ± 1.32 nm). In effect, the more material adsorbed onto the shell, the lower the roughness. 3D renderings of these coated cells are shown in Fig. 15a-e, and correspond with the sample designations in Fig. 14a-e. RMS roughness as measured by AFM is shown in Fig. 16. Initial microroughness of 4 nm for bare cell surface increases to 9 nm for one bilayer but decreases to 3.5 nm for two bilayers deposited from higher concentration solution. The resulting smoothed surface is evidence of uniform, conformal and homogeneous LbL coatings on the cells if thickness increased beyond 5 nm.

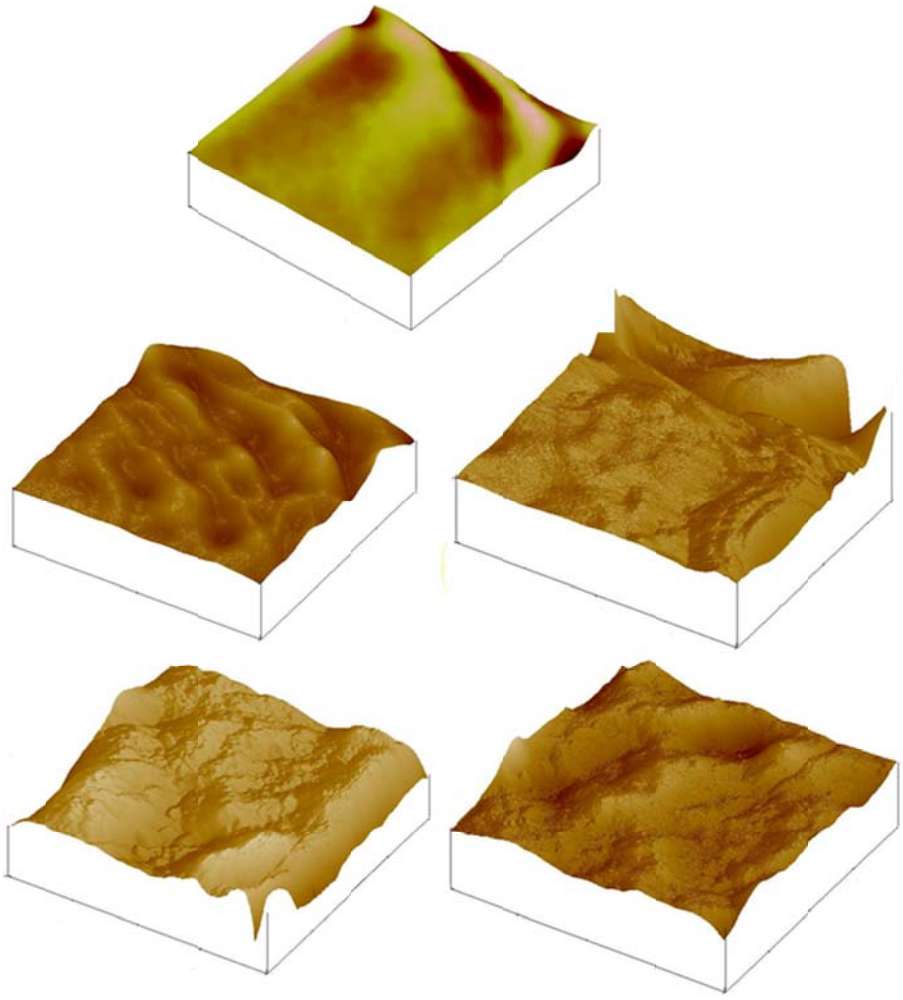

Figure 15: 3D topographical AFM images of of (a) bare and (b)-(e) coated YPH501 yeast cells. Scale is 2 µm x 2µm. (b) 1 bilayer, 0.5 mg/mL; (c) 1 bilayer, 2 mg/mL; (d) 2 bilayers, 0.5 mg/mL; (e) 2 bilayers, 2 mg/mL.

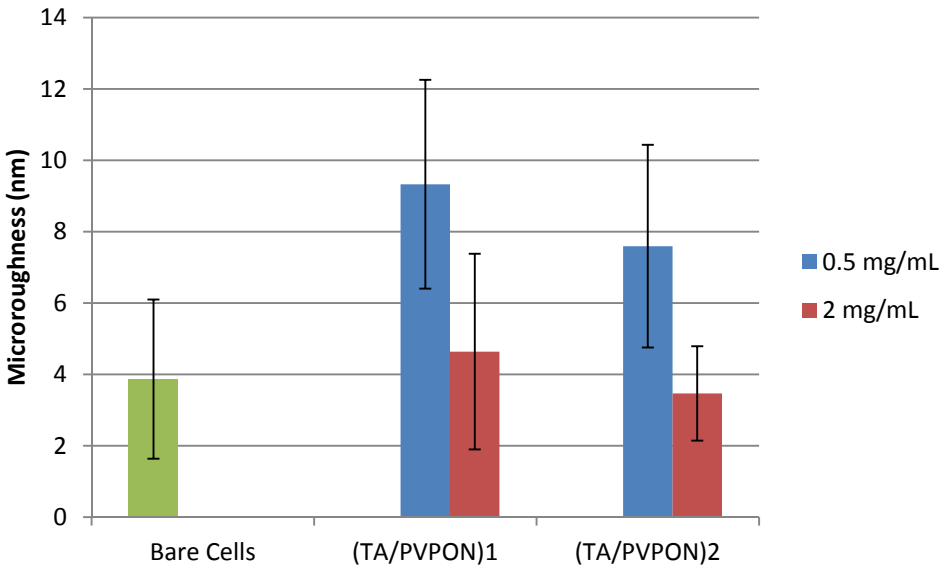

Figure 16: RMS roughness measurements as calculated by AFM

The absence of cationic pre-layer during LbL assembly caused little change in the surface charge of the cells in contrast to previous studies with PEI pre-layer (Fig. 17). ζ potential remains the nearly constant (around -50 mV) and varies very little after deposition of each layer thus confirming that hydrogen bonded assembly does not change initial potential. It is worth noting that maintaining a constant, high ζ-potential on cell surfaces results in good cell suspension stability and prevents severe aggregation which further simplifies the formation of uniform cell layers and study of their viability.[33]

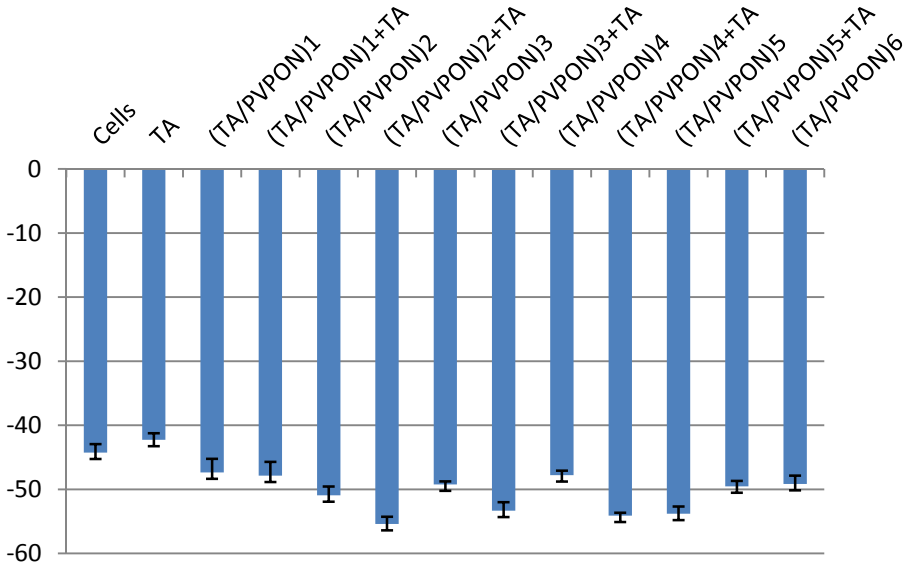

Figure 17: ζ-potential of encapsulated yeast cells at pH 6

Encapsulated Cell Viability & Growth

Procedure

Encapsulated cells were incubated in 2% raffinose and 2% galactose in SMM yeast media at 30 ºC to induce the yEGFP production. Optical density at 600 nm (OD600) and fluorescence were measured at indicated time points to assess cell growth.

Evaluation

The viability of encapsulated cells was assessed with the resazurin assay.[55] Bioreduction of resazurin is achieved by reducing enzyme cofactors in viable cells and results in the conversion of resazurin's oxidized blue form to its pink fluorescent intermediate, resorufin.[56] The absence of such cofactors in dead cells leads to no conversion and no fluorescence can be detected.[57]

Cells coated with (TA/PVPON) layers showed viability exceeding that of PEI(TA/PVPON)-coated cells when comparing a number of variables. Fig. 18 shows viability of cells encapsulated with and without PEI, with different molecular weights of PVPON (360 kDa or 1 300 kDa), and with different numbers of TA/PVPON bilayers (two or four).

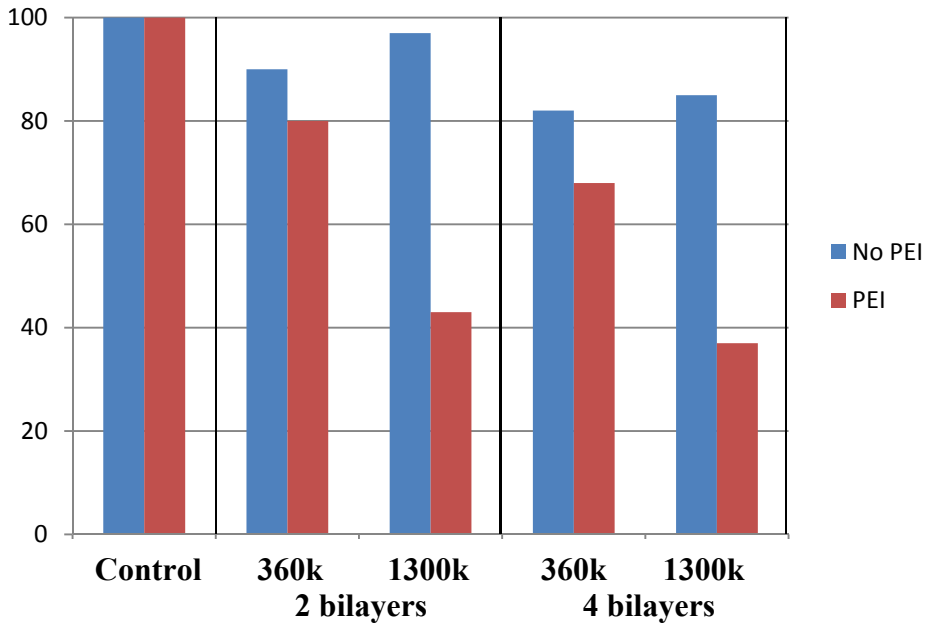

Figure 18: Comparison of encapsulated yeast cell viability (%) for cells encapsulated with and without PEI as measured by resazurin assay.

When comparing viability of cells encapsulated with and without PEI pre-layer, those without PEI outperform those with PEI in all cases: for two and four bilayer shells and different molecular weights of PVPON component. The highest viability was recorded for cells encapsulated with two bilayer shells with the highest molecular weight of PVPON component, reaching 94% vs those with PEI pre-layer with only 42% (Fig. 18). For four bilayer shells, the viability slightly decreased to 85% but still remains much higher than that for shells with cationic PEI component. It is worth noting that higher

molecular weight PVPON component promoted cell viability in the case of truly non-ionic shells in contrast to shells assembled with PEI pre-layer.

To estimate the permeability of low molecular weight molecules through hollow (TA/PVPON) capsules, the diffusion of FITC was measured by FRAP as described in the methods section.

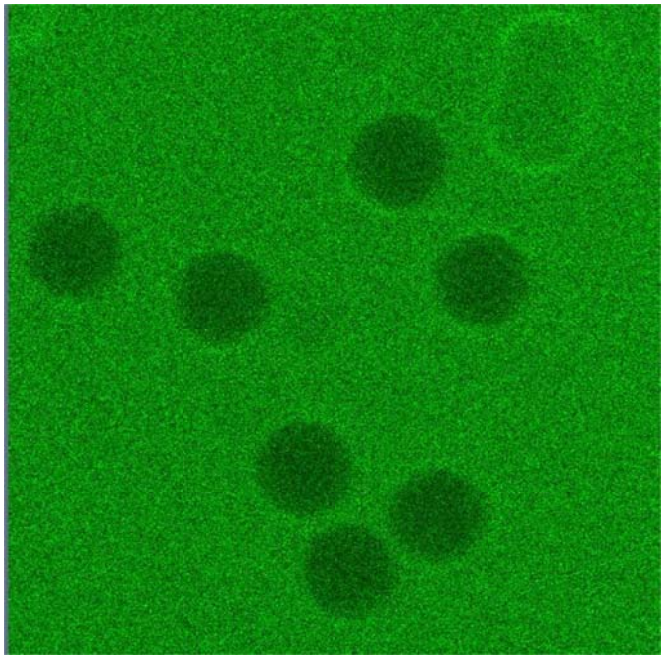

Figure 19: CLSM image of photobleached hollow capsules used for FRAP measurements

The fluorescence intensity I(t) of photobleached hollow capsules, like those shown in Fig. 19, was measured using ImageJ software and plotted as a function of time. Using Origin, a first-order exponential decay fit was performed to determine the coefficient A from the fit equation. The diffusion coefficient D was then calculated using $A = 3D/rh$, where r is capsule radius and h is capsule height. Two sample plots and their fits are shown in Fig. 20.

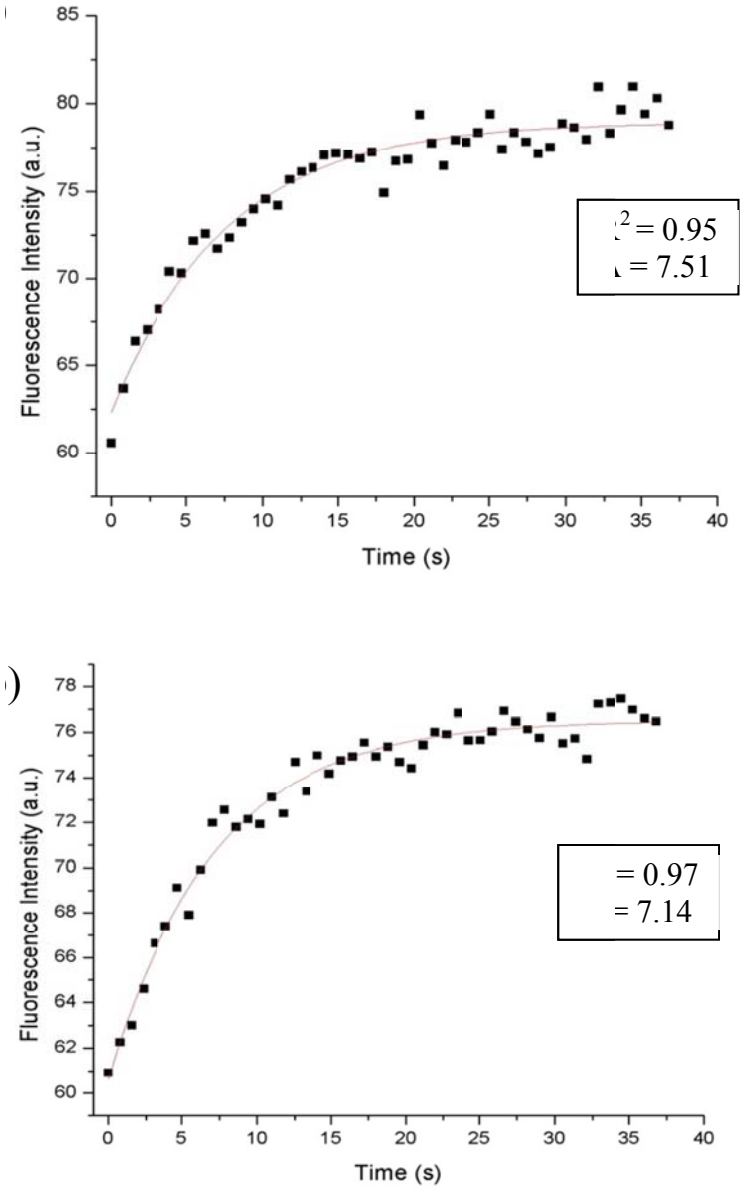

Figure 20: Fluorescence intensity recovery plots (I(t) vs. time) for (a) $(TA/PVPON)_6$ and (b) $PEI(TA/PVPON)_6$ hollow capsules

(TA/PVPON) shells display a diffusion coefficient approximately 1.5x higher than electrostatically-bonded (PAH/PSS) shells, but about 2x *lower* than hydrogen-bonded PEI(TA/PVPON) shells (Fig. 21). We attribute these differences to differences in bonding between polymers, which also have an effect on the thickness of the polymer shells (Fig. 22).

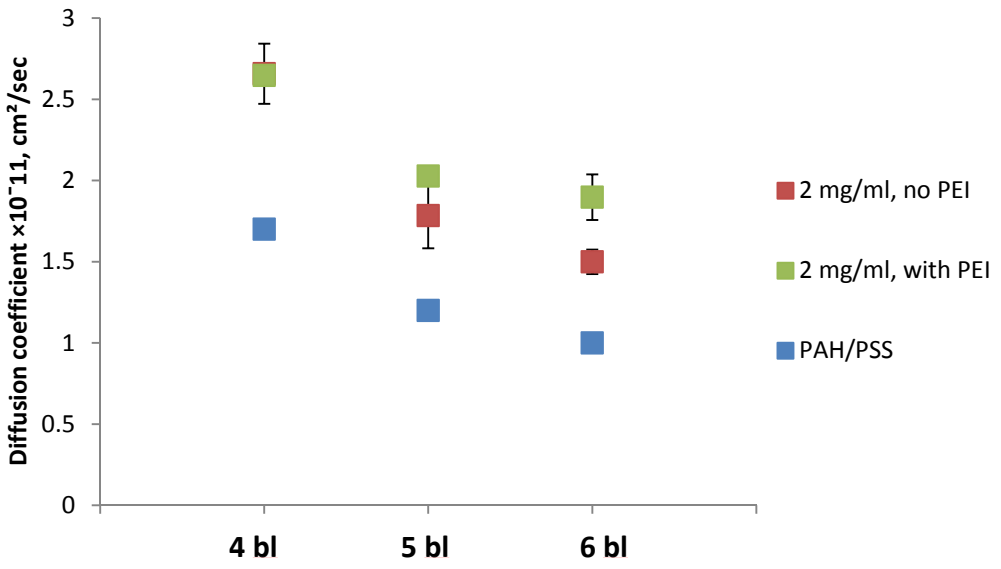

Figure 21: Comparison of diffusion coefficient of cells encapsulated with (PAH/PSS), PEI(TA/PVPON), and (TA/PVPON).

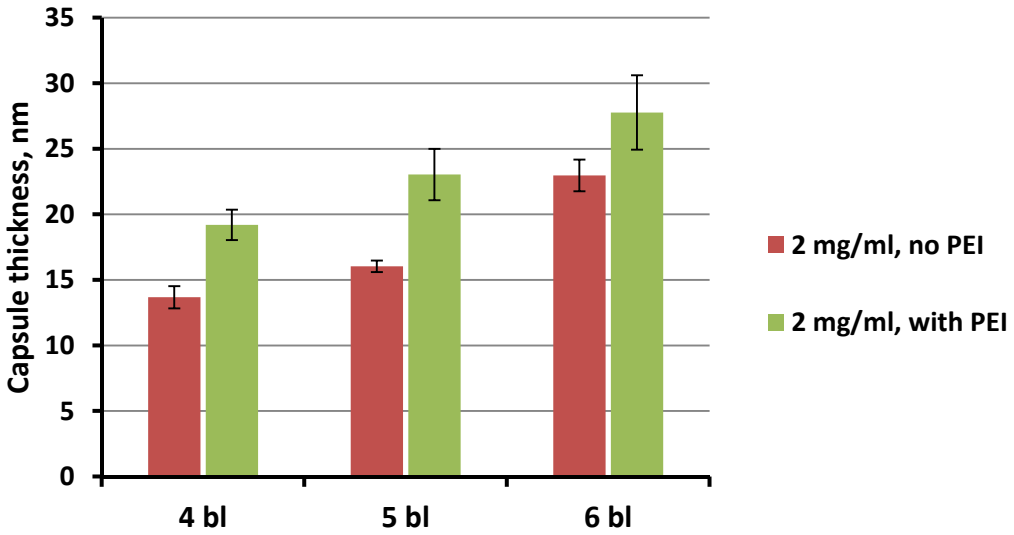

Figure 22: Thickness of collapsed hollow capsules as determined via AFM height measurements.

The higher thickness of shells constructed using PEI would lead one to assume that the rate of diffusion through these shells would be lower than those constructed without PEI. However, we see the opposite effect in our study. This can be attributed to

the effect the PEI pre-layer has on the interatomic bonding behavior of TA and PVPON, illustrated in Fig. 23.

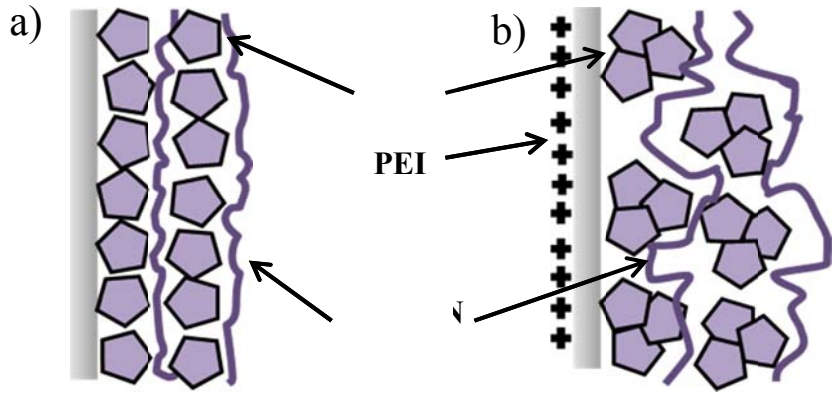

Figure 23: Schematic of interatomic bonding behavior of (a) truly non-ionic hydrogen-bonded shells, and (b) PEI-primed hydrogen-bonded shells

Positively charged PEI-treated surfaces result in thicker shells due to tannic acid aggregation. Tannic acid has been shown to aggregate with its LbL counterpart (in this case, PVPON) in hollow LbL shells.[33,58] These aggregates give rise to the loose, grainy morphology of PEI(TA/PVPON) shells noted previously.[33] In contrast, the hydrogen bonds between layers of PEI-free shells produce more densely packed shells. Although the individual hydrogen bonds in this structure are weak, collectively they are a strong barrier to FITC diffusion. This, in combination with the dense network the small FITC molecules have to navigate, result in a lower diffusion coefficient for (TA/PVPON) shells when compared to PEI(TA/PVPON) shells.

Cells' ability to proliferate and express green fluorescent protein (GFP) after encapsulation was indicative of preserved function. GFP expression is induced by the addition of small molecule galactose (Gal) to our *S. cerevisiae* yeast cells with

incorporated GFP reporters. GFP expression is determined by normalizing fluorescence of expressed GFP to cell density as measured by optical density (OD600). Fig. 24 shows the fluorescence intensity of cells incubated with and without galactose. Those without galactose do not express GFP.

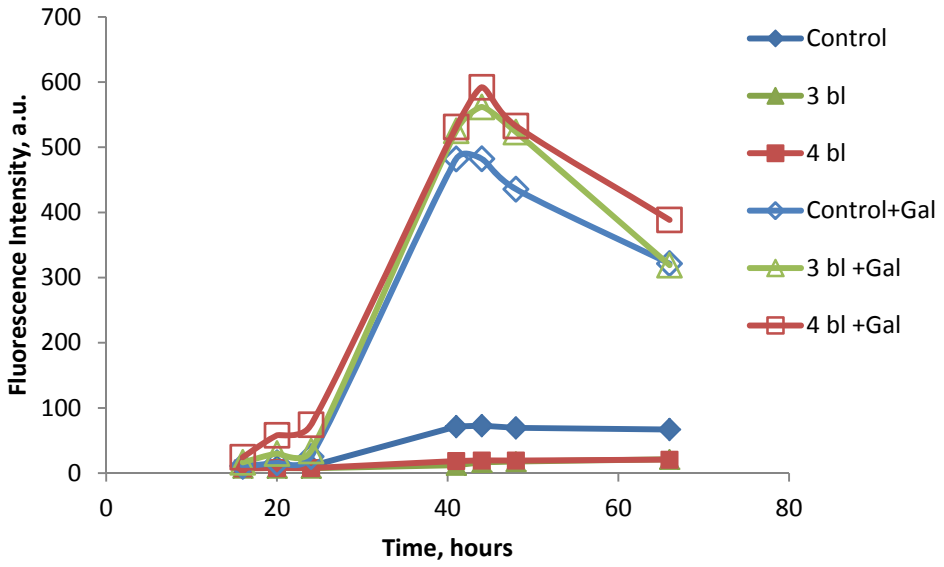

Figure 24: GFP expression of cells encapsulated with and without galactose

The characteristic S-shaped growth curves of control cells, PEI(TA/PVPON)-coated cells, and (TA/PVPON)-coated cells are shown in Fig. 24. To monitor cell growth, we measure optical density (OD600) of cell suspensions. During the initial lag phase, cell division (growth rate) is slow in all cases. This stage is followed by the exponential growth mode, where cell division accelerates and a unicellular organism duplicates, i.e., one cell produces two in a given period of time. The exponential phase then proceeds to a stationary phase when there is no discernible change in cell concentration.

As shown in our previous studies, there is a delay of the exponential phase for the PEI(TA/PVPON)-coated cells, as compared to bare yeast cells, which is dependent on the

thickness of the polymer coating (Fig. 25a). In contrast, no delay in cell growth is shown for (TA/PVPON)-coated cells, no matter the thickness of the coating (Fig. 25b). Similarly, GFP expression is delayed in cells encapsulated with PEI, and there is no delay in expression for cell encapsulated without PEI (Fig. 26).

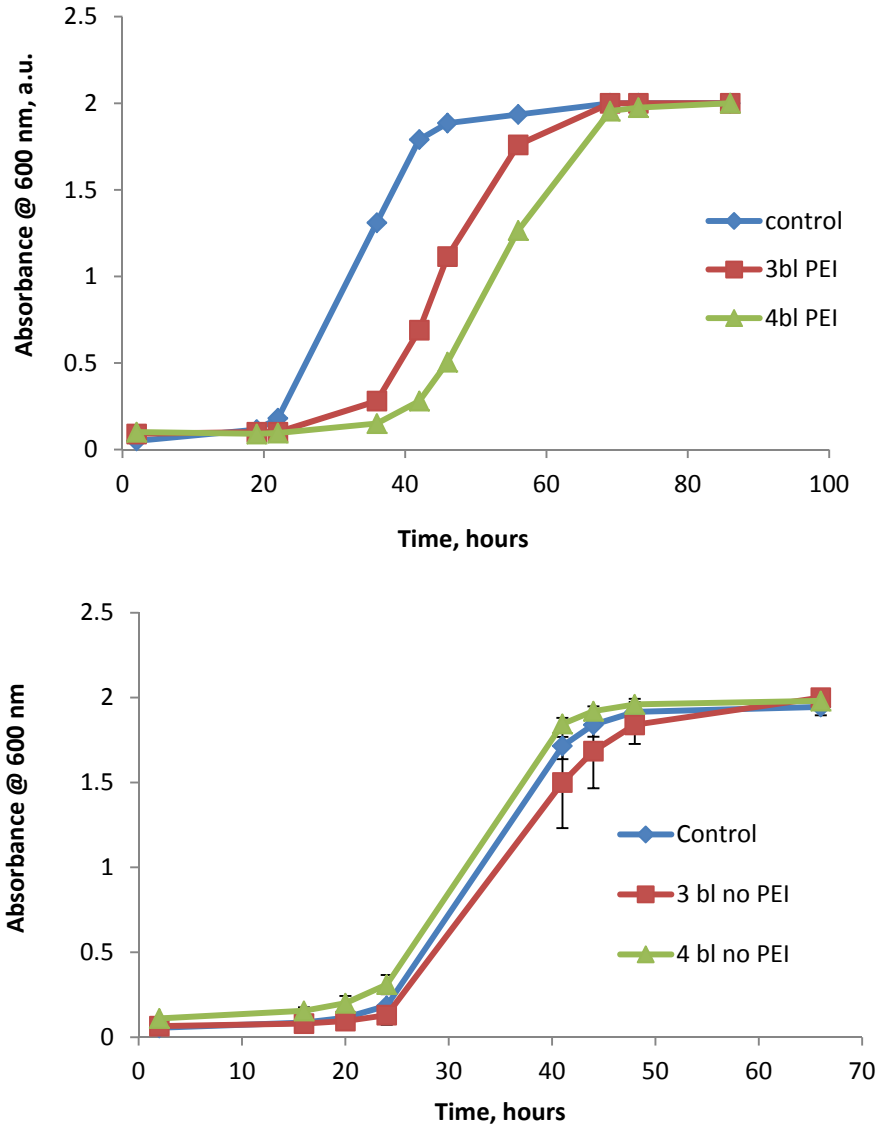

Figure 25: Characteristic s-shaped cell growth as measured by OD600. (a) Cells encapsulated with cationic precursor PEI show delayed entrance into exponential phase, while (b) cells encapsulated with no precursor show no delay of cell growth.

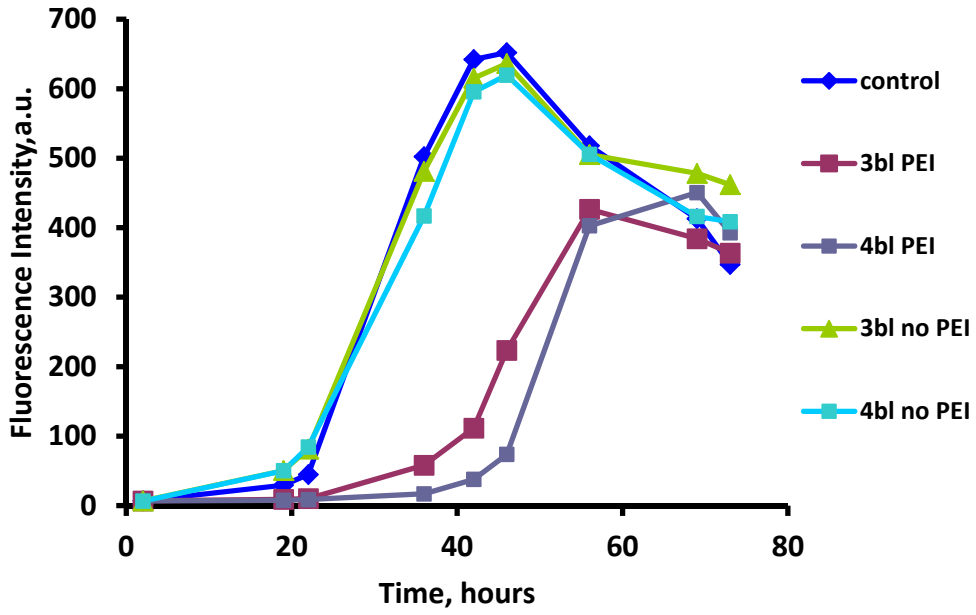

Figure 26: GFP expression of cells encapsulated with and without PEI

We expected to see the opposite result here due to the higher diffusion coefficient of shells constructed with PEI. The explanation for this apparent contradiction lies in the mechanical stability of the polymer shells. Cells encapsulated in PEI(TA/PVPON) actually begin to divide within the polymer shell. Their loose, grainy morphology allows for stretching, and thus can accommodate a budding cell. When the daughter cell is large enough, the polymer shell is ruptured. Thicker shells (more bilayers) take longer for cells to break through, and consequently delay the growth curve of PEI(TA/PVPON)-coated cells. In contrast, dense, tightly packed (TA/PVPON) shells are easily ruptured by dividing cells, and therefore show no delay in the growth curve.

CHAPTER 5

CONCLUSIONS

Herein we discuss the benefits of hydrogen-bonded LbL shells as compared to electrostatically-bonded LbL shells and to other methods of encapsulation. Electrostatically-bonded LbL components demonstrate extreme cytotoxicity and limit diffusion of nutrients into the cell. We report on an improved strategy for cell surface modification through LbL assembly of truly non-ionic nanoscale hydrogen-bonded shells. The elimination of the polycation PEI as a pre-layer allows encapsulated cells to maintain a high viability (94%) as compared to cells encapsulated with the cationic pre-layer (74%). This high cytocompatibility is a result of the cells having no exposure to the cytotoxic polycations once presumed necessary for shell construction, and from the high permeability of the shells. Their permeability allows for easy penetration of nutrients to the cell interior. Additionally, the mechanical stability of the non-ionic shells is such that the shell shape is maintained, but can be ruptured by dividing cells.

A potential next step in this area of research is to verify that these truly non-ionic LbL shells do indeed possess tunable permeability by measuring changes in the diffusion coefficient with pH variation. Evaluating the cell storage capability of the shells by monitoring how long encapsulated cells remain viable will also be beneficial. It is likely that these truly non-ionic shells will not display the same storage properties as shells utilizing the PEI pre-layer, since the mechanical stability of the former allows for easy rupture by dividing cells.

This research contributes to the fields of materials and polymer science by communicating new knowledge about physical and chemical mechanisms to

functionalize cell membranes. These methods for molecular design of materials can serve as the building blocks for assembling responsive artificial cell membranes, which then facilitate an understanding of responsive cell membranes' potential capabilities in polymer-based regulation of cell viability and role in easing cell integration into synthetic functional matrices. This research is applicable to designing polymer-based cell coatings which aid in the protection, prolonged storage, and controlled delivery of cells. It is also a step toward development of robust engineered synthetic cell systems. The fields of biomedical and biosensing sciences stand to benefit from living cell surface engineering utilizing non-cytotoxic, potentially stimulus-responsive LbL components.

REFERENCES

1. Raymond, M. C.; Neufeld, R. J.; Poncelet, D., Encapsulation of brewers yeast in chitosan coated carrageenan microspheres by emulsification/thermal gelation. *Artif Cells Blood Substit Immobil Biotechnol* **2004,** *32* (2), 275-91.

2. Wilson, J. T.; Chaikof, E. L., Challenges and emerging technologies in the immunoisolation of cells and tissues. *Adv Drug Deliv Rev* **2008,** *60* (2), 124-45.

3. Caruso, F.; Trau, D.; Möhwald, H.; Renneberg, R., Enzyme Encapsulation in Layer-by-Layer Engineered Polymer Multilayer Capsules. *Langmuir* **2000,** *16* (4), 1485-1488.

4. Orive, G.; Hernandez, R. M.; Gascon, A. R.; Calafiore, R.; Chang, T. M. S.; Vos, P. D.; Hortelano, G.; Hunkeler, D.; Lacik, I.; Shapiro, A. M. J.; Pedraz, J. L., Cell encapsulation: Promise and progress. *Nat Med* **2003,** *9* (1), 104-107.

5. Tang, Z.; Wang, Y.; Podsiadlo, P.; Kotov, N. A., Biomedical Applications of Layer-by-Layer Assembly: From Biomimetics to Tissue Engineering. *Advanced Materials* **2006,** *18* (24), 3203-3224.

6. Sukhorukov, G. B.; Moehwald, H., Polyelectrolyte Microcapsules as Biomimetic Assemblies. In *Colloids and Colloid Assemblies*, Caruso, F., Ed. 2004.

7. Yu, L.; Ding, J., Injectable hydrogels as unique biomedical materials. *Chemical Society Reviews* **2008,** *37* (8), 1473-1481.

8. Xu, Y.; Jang, K.; Konno, T.; Ishihara, K.; Mawatari, K.; Kitamori, T., The biological performance of cell-containing phospholipid polymer hydrogels in bulk and microscale form. *Biomaterials* **2010,** *31* (34), 8839-8846.

9. Nuttelman, C. R.; Rice, M. A.; Rydholm, A. E.; Salinas, C. N.; Shah, D. N.; Anseth, K. S., Macromolecular monomers for the synthesis of hydrogel niches and their application in cell encapsulation and tissue engineering. *Progress in Polymer Science* **2008,** *33* (2), 167-179.

10. Hennink, W. E.; van Nostrum, C. F., Novel crosslinking methods to design hydrogels. *Adv Drug Deliv Rev* **2002,** *54* (1), 13-36.

11. Teramura, Y.; Iwata, H., Cell surface modification with polymers for biomedical studies. *Soft Matter* **2010,** *6* (6), 1081-1091.

12. Yun Lee, D.; Hee Nam, J.; Byun, Y., Functional and histological evaluation of transplanted pancreatic islets immunoprotected by PEGylation and cyclosporine for 1 year. *Biomaterials* **2007,** *28* (11), 1957-1966.

13. Cabric, S.; Sanchez, J.; Lundgren, T.; Foss, A.; Felldin, M.; Kallen, R.; Salmela, K.; Tibell, A.; Tufveson, G.; Larsson, R.; Korsgren, O.; Nilsson, B., Islet surface heparinization prevents the instant blood-mediated inflammatory reaction in islet transplantation. *Diabetes* **2007,** *56* (8), 2008-15.

14. Teramura, Y.; Kaneda, Y.; Totani, T.; Iwata, H., Behavior of synthetic polymers immobilized on a cell membrane. *Biomaterials* **2008,** *29* (10), 1345-55.

15. Rabuka, D.; Forstner, M. B.; Groves, J. T.; Bertozzi, C. R., Noncovalent cell surface engineering: incorporation of bioactive synthetic glycopolymers into cellular membranes. *J Am Chem Soc* **2008,** *130* (18), 5947-53.

16. Paulick, M. G.; Forstner, M. B.; Groves, J. T.; Bertozzi, C. R., A chemical approach to unraveling the biological function of the glycosylphosphatidylinositol anchor. *Proc Natl Acad Sci U S A* **2007,** *104* (51), 20332-7.

17. Teramura, Y.; Kaneda, Y.; Iwata, H., Islet-encapsulation in ultra-thin layer-by-layer membranes of poly(vinyl alcohol) anchored to poly(ethylene glycol)-lipids in the cell membrane. *Biomaterials* **2007,** *28* (32), 4818-25.

18. Diaspro, A.; Silvano, D.; Krol, S.; Cavalleri, O.; Gliozzi, A., Single Living Cell Encapsulation in Nano-organized Polyelectrolyte Shells. *Langmuir* **2002,** *18* (13), 5047-5050.

19. Hammond, P. T., Form and function in multilayer assembly: New applications at the nanoscale. *Adv. Mater. (Weinheim, Ger.)* **2004,** *16* (Copyright (C) 2011 American Chemical Society (ACS). All Rights Reserved.), 1271-1293.

20. Quinn, J. F.; Johnston, A. P. R.; Such, G. K.; Zelikin, A. N.; Caruso, F., Next generation, sequentially assembled ultrathin films: beyond electrostatics. *Chem. Soc. Rev.* **2007,** *36* (Copyright (C) 2011 American Chemical Society (ACS). All Rights Reserved.), 707-718.

21. del Mercato, L. L.; Rivera-Gil, P.; Abbasi, A. Z.; Ochs, M.; Ganas, C.; Zins, I.; Sonnichsen, C.; Parak, W. J., LbL multilayer capsules: recent progress and future outlook for their use in life sciences. *Nanoscale* **2010,** *2* (4), 458-67.

22. Hoffman, A. S., Hydrogels for biomedical applications. *Adv Drug Deliv Rev* **2002,** *54* (1), 3-12.

23. Zelikin, A. N.; Becker, A. L.; Johnston, A. P. R.; Wark, K. L.; Turatti, F.; Caruso, F., A General Approach for DNA Encapsulation in Degradable Polymer Microcapsules. *ACS Nano* **2007,** *1* (Copyright (C) 2011 American Chemical Society (ACS). All Rights Reserved.), 63-69.

24. Zelikin, A. N.; Li, Q.; Caruso, F., Disulfide-Stabilized Poly(methacrylic acid) Capsules: Formation, Cross-Linking, and Degradation Behavior. *Chem. Mater.* **2008,** *20* (Copyright (C) 2011 American Chemical Society (ACS). All Rights Reserved.), 2655-2661.

25. Kozlovskaya, V.; Kharlampieva, E.; Erel, I.; Sukhishvili, S. A., Multilayer-derived, ultrathin, stimuli-responsive hydrogels. *Soft Matter* **2009,** *5* (Copyright (C) 2011 American Chemical Society (ACS). All Rights Reserved.), 4077-4087.

26. Kinnane, C. R.; Such, G. K.; Antequera-Garcia, G.; Yan, Y.; Dodds, S. J.; Liz-Marzan, L. M.; Caruso, F., Low-Fouling Poly(N-vinyl pyrrolidone) Capsules with Engineered Degradable Properties. *Biomacromolecules* **2009,** *10* (Copyright (C) 2011 American Chemical Society (ACS). All Rights Reserved.), 2839-2846.

27. De Koker, S.; De Geest, B. G.; Cuvelier, C.; Ferdinande, L.; Deckers, W.; Hennink, W. E.; De Smedt, S. C.; Mertens, N., In vivo Cellular Uptake, Degradation, and Biocompatibility of Polyelectrolyte Microcapsules. *Advanced Functional Materials* **2007,** *17* (18), 3754-3763.

28. Stadler, B.; Chandrawati, R.; Price, A. D.; Chong, S. F.; Breheney, K.; Postma, A.; Connal, L. A.; Zelikin, A. N.; Caruso, F., A microreactor with thousands of subcompartments: enzyme-loaded liposomes within polymer capsules. *Angew Chem Int Ed Engl* **2009,** *48* (24), 4359-62.

29. Bieber, T.; Meissner, W.; Kostin, S.; Niemann, A.; Elsasser, H. P., Intracellular route and transcriptional competence of polyethylenimine-DNA complexes. *J Control Release* **2002,** *82* (2-3), 441-54.

30. Godbey, W. T.; Wu, K. K.; Mikos, A. G., Size matters: molecular weight affects the efficiency of poly(ethylenimine) as a gene delivery vehicle. *J Biomed Mater Res* **1999,** *45* (3), 268-75.

31. Germain, M.; Balaguer, P.; Nicolas, J.-C.; Lopez, F.; Esteve, J.-P.; Sukhorukov, G. B.; Winterhalter, M.; Richard-Foy, H.; Fournier, D., Protection of mammalian cell used in biosensors by coating with a polyelectrolyte shell. *Biosensors and Bioelectronics* **2006,** *21* (8), 1566-1573.

32. Fakhrullin, R. F.; Zamaleeva, A. I.; Morozov, M. V.; Tazetdinova, D. I.; Alimova, F. K.; Hilmutdinov, A. K.; Zhdanov, R. I.; Kahraman, M.; Culha, M., Living Fungi Cells Encapsulated in Polyelectrolyte Shells Doped with Metal Nanoparticles. *Langmuir* **2009,** *25* (8), 4628-4634.

33. Kozlovskaya, V.; Harbaugh, S.; Drachuk, I.; Shchepelina, O.; Kelley-Loughnane, N.; Stone, M.; Tsukruk, V. V., Hydrogen-bonded LbL shells for living cell surface engineering. *Soft Matter* **2011**, *7* (6), 2364-2372.

34. Kharlampieva, E.; Kozlovskaya, V.; Sukhishvili, S. A., Layer-by-Layer Hydrogen-Bonded Polymer Films: From Fundamentals to Applications. *Advanced Materials* **2009,** *21* (30), 3053-3065.

35. Kozlovskaya, V.; Kharlampieva, E.; Drachuk, I.; Cheng, D.; Tsukruk, V. V., Responsive microcapsule reactors based on hydrogen-bonded tannic acid layer-by-layer assemblies. *Soft Matter* **2010,** *6* (15), 3596-3608.

36. Such, G. K.; Johnston, A. P. R.; Caruso, F., Engineered hydrogen-bonded polymer multilayers: from assembly to biomedical applications. *Chemical Society Reviews* **2011,** *40* (1), 19-29.

37. Erel-Unal, I.; Sukhishvili, S. A., Hydrogen-Bonded Multilayers of a Neutral Polymer and a Polyphenol. *Macromolecules* **2008,** *41* (11), 3962-3970.

38. Hushpulian, D. M.; Fechina, V. A.; Kazakov, S. V.; Sakharov, I. Y.; Gazaryan, I. G., Non-enzymatic interaction of reaction products and substrates in peroxidase catalysis. *Biochemistry (Mosc)* **2003,** *68* (9), 1006-11.

39. Takebayashi, J.; Tai, A.; Yamamoto, I., pH-dependent long-term radical scavenging activity of AA-2G and 6-Octa-AA-2G against 2,2'-azinobis(3-ethylbenzothiazoline-6-sulfonic acid) radical cation. *Biol Pharm Bull* **2003,** *26* (9), 1368-70.

40. Shutova, T.; Agabekov, V.; Lvov, Y., Reaction of radical cations with multilayers of tannic acid and polyelectrolytes. *Russian Journal of General Chemistry* **2007,** *77* (9), 1494-1501.

41. Kozlovskaya, V.; Yakovlev, S.; Libera, M.; Sukhishvili, S. A., Surface Priming and the Self-Assembly of Hydrogen-Bonded Multilayer Capsules and Films. *Macromolecules* **2005,** *38* (11), 4828-4836.

42. Koper, G. J. M.; van Duijvenbode, R. C.; Stam, D. D. P. W.; Steuerle, U.; Borkovec, M., Synthesis and Protonation Behavior of Comblike Poly(ethyleneimine). *Macromolecules* **2003,** *36* (7), 2500-2507.

43. Mészáros, R.; Thompson, L.; Bos, M.; de Groot, P., Adsorption and Electrokinetic Properties of Polyethylenimine on Silica Surfaces. *Langmuir* **2002,** *18* (16), 6164-6169.

44. Brunot, C.; Ponsonnet, L.; Lagneau, C.; Farge, P.; Picart, C.; Grosgogeat, B., Cytotoxicity of polyethyleneimine (PEI), precursor base layer of polyelectrolyte multilayer films. *Biomaterials* **2007,** *28* (4), 632-40.

45. Tsukruk, V. V.; Reneker, D. H., Scanning probe microscopy of organic and polymeric films: from self-assembled monolayers to composite multilayers. *Polymer* **1995,** *36* (9), 1791-1808.

46. Glinel, K.; Sukhorukov, G. B.; Möhwald, H.; Khrenov, V.; Tauer, K., Thermosensitive Hollow Capsules Based on Thermoresponsive Polyelectrolytes. *Macromolecular Chemistry and Physics* **2003,** *204* (14), 1784-1790.

47. Contributers, W. Fluorescence recovery after photobleaching. http://en.wikipedia.org/w/index.php?title=Fluorescence_recovery_after_photobleaching&oldid=406389463 (accessed 28 February).

48. Ibarz, G.; Dähne, L.; Donath, E.; Möhwald, H., Controlled Permeability of Polyelectrolyte Capsules via Defined Annealing. *Chemistry of Materials* **2002,** *14* (10), 4059-4062.

49. Glinel, K.; Dubois, M.; Verbavatz, J. M.; Sukhorukov, G. B.; Zemb, T., Determination of pore size of catanionic icosahedral aggregates. *Langmuir* **2004,** *20* (20), 8546-51.

50. Antipov, A. A.; Sukhorukov, G. B.; Donath, E.; Möhwald, H., Sustained Release Properties of Polyelectrolyte Multilayer Capsules. *The Journal of Physical Chemistry B* **2001,** *105* (12), 2281-2284.

51. Shutava, T. G.; Balkundi, S. S.; Vangala, P.; Steffan, J. J.; Bigelow, R. L.; Cardelli, J. A.; O'Neal, D. P.; Lvov, Y. M., Layer-by-Layer-Coated Gelatin Nanoparticles as a Vehicle for Delivery of Natural Polyphenols. *ACS Nano* **2009**.

52. Riedl, K. M.; Hagerman, A. E., Tannin-protein complexes as radical scavengers and radical sinks. *J Agric Food Chem* **2001,** *49* (10), 4917-23.

53. Lopes, G. K.; Schulman, H. M.; Hermes-Lima, M., Polyphenol tannic acid inhibits hydroxyl radical formation from Fenton reaction by complexing ferrous ions. *Biochim Biophys Acta* **1999,** *1472* (1-2), 142-52.

54. Sherman, F., Getting started with yeast. *Methods Enzymol* **2002,** *350*, 3-41.

55. Dutka, B. J.; Nyholm, N.; Petersen, J., Comparison of several microbiological toxicity screening tests. *Water Research* **1983,** *17* (10), 1363-1368.

56. Strotmann, U. J.; Butz, B.; Bias, W. R., The dehydrogenase assay with resazurin: practical performance as a monitoring system and Ph-dependent toxicity of phenolic compounds. *Ecotoxicol Environ Saf* **1993,** *25* (1), 79-89.

57. Mak, W. C.; Sum, K. W.; Trau, D.; Renneberg, R., Nanoscale surface engineered living cells with extended substrate spectrum. *IEE Proc Nanobiotechnol* **2004,** *151* (2), 67-72.

58. Shutava, T.; Prouty, M.; Kommireddy, D.; Lvov, Y., pH Responsive Decomposable Layer-by-Layer Nanofilms and Capsules on the Basis of Tannic Acid. *Macromolecules* **2005,** *38* (7), 2850-2858.

1. Raymond, M. C.; Neufeld, R. J.; Poncelet, D., Encapsulation of brewers yeast in chitosan coated carrageenan microspheres by emulsification/thermal gelation. *Artif Cells Blood Substit Immobil Biotechnol* **2004,** *32* (2), 275-91.
2. Wilson, J. T.; Chaikof, E. L., Challenges and emerging technologies in the immunoisolation of cells and tissues. *Adv Drug Deliv Rev* **2008,** *60* (2), 124-45.
3. Caruso, F.; Trau, D.; Möhwald, H.; Renneberg, R., Enzyme Encapsulation in Layer-by-Layer Engineered Polymer Multilayer Capsules. *Langmuir* **2000,** *16* (4), 1485-1488.
4. Orive, G.; Hernandez, R. M.; Gascon, A. R.; Calafiore, R.; Chang, T. M. S.; Vos, P. D.; Hortelano, G.; Hunkeler, D.; Lacik, I.; Shapiro, A. M. J.; Pedraz, J. L., Cell encapsulation: Promise and progress. *Nat Med* **2003,** *9* (1), 104-107.
5. Tang, Z.; Wang, Y.; Podsiadlo, P.; Kotov, N. A., Biomedical Applications of Layer-by-Layer Assembly: From Biomimetics to Tissue Engineering. *Advanced Materials* **2006,** *18* (24), 3203-3224.
6. Sukhorukov, G. B.; Moehwald, H., Polyelectrolyte Microcapsules as Biomimetic Assemblies. In *Colloids and Colloid Assemblies*, Caruso, F., Ed. 2004.
7. Yu, L.; Ding, J., Injectable hydrogels as unique biomedical materials. *Chemical Society Reviews* **2008,** *37* (8), 1473-1481.
8. Xu, Y.; Jang, K.; Konno, T.; Ishihara, K.; Mawatari, K.; Kitamori, T., The biological performance of cell-containing phospholipid polymer hydrogels in bulk and microscale form. *Biomaterials* **2010,** *31* (34), 8839-8846.
9. Nuttelman, C. R.; Rice, M. A.; Rydholm, A. E.; Salinas, C. N.; Shah, D. N.; Anseth, K. S., Macromolecular monomers for the synthesis of hydrogel niches and their application in cell encapsulation and tissue engineering. *Progress in Polymer Science* **2008,** *33* (2), 167-179.
10. Hennink, W. E.; van Nostrum, C. F., Novel crosslinking methods to design hydrogels. *Adv Drug Deliv Rev* **2002,** *54* (1), 13-36.
11. Teramura, Y.; Iwata, H., Cell surface modification with polymers for biomedical studies. *Soft Matter* **2010,** *6* (6), 1081-1091.

12. Yun Lee, D.; Hee Nam, J.; Byun, Y., Functional and histological evaluation of transplanted pancreatic islets immunoprotected by PEGylation and cyclosporine for 1 year. *Biomaterials* **2007,** *28* (11), 1957-1966.
13. Cabric, S.; Sanchez, J.; Lundgren, T.; Foss, A.; Felldin, M.; Kallen, R.; Salmela, K.; Tibell, A.; Tufveson, G.; Larsson, R.; Korsgren, O.; Nilsson, B., Islet surface heparinization prevents the instant blood-mediated inflammatory reaction in islet transplantation. *Diabetes* **2007,** *56* (8), 2008-15.
14. Rabuka, D.; Forstner, M. B.; Groves, J. T.; Bertozzi, C. R., Noncovalent cell surface engineering: incorporation of bioactive synthetic glycopolymers into cellular membranes. *J Am Chem Soc* **2008,** *130* (18), 5947-53.
15. Paulick, M. G.; Forstner, M. B.; Groves, J. T.; Bertozzi, C. R., A chemical approach to unraveling the biological function of the glycosylphosphatidylinositol anchor. *Proc Natl Acad Sci U S A* **2007,** *104* (51), 20332-7.
16. Teramura, Y.; Kaneda, Y.; Iwata, H., Islet-encapsulation in ultra-thin layer-by-layer membranes of poly(vinyl alcohol) anchored to poly(ethylene glycol)-lipids in the cell membrane. *Biomaterials* **2007,** *28* (32), 4818-25.
17. Diaspro, A.; Silvano, D.; Krol, S.; Cavalleri, O.; Gliozzi, A., Single Living Cell Encapsulation in Nano-organized Polyelectrolyte Shells. *Langmuir* **2002,** *18* (13), 5047-5050.
18. Hammond, P. T., Form and function in multilayer assembly: New applications at the nanoscale. *Adv. Mater. (Weinheim, Ger.)* **2004,** *16* (Copyright (C) 2011 American Chemical Society (ACS). All Rights Reserved.), 1271-1293.
19. Quinn, J. F.; Johnston, A. P. R.; Such, G. K.; Zelikin, A. N.; Caruso, F., Next generation, sequentially assembled ultrathin films: beyond electrostatics. *Chem. Soc. Rev.* **2007,** *36* (Copyright (C) 2011 American Chemical Society (ACS). All Rights Reserved.), 707-718.
20. del Mercato, L. L.; Rivera-Gil, P.; Abbasi, A. Z.; Ochs, M.; Ganas, C.; Zins, I.; Sonnichsen, C.; Parak, W. J., LbL multilayer capsules: recent progress and future outlook for their use in life sciences. *Nanoscale* **2010,** *2* (4), 458-67.
21. Hoffman, A. S., Hydrogels for biomedical applications. *Adv Drug Deliv Rev* **2002,** *54* (1), 3-12.
22. Zelikin, A. N.; Becker, A. L.; Johnston, A. P. R.; Wark, K. L.; Turatti, F.; Caruso, F., A General Approach for DNA Encapsulation in Degradable Polymer Microcapsules. *ACS Nano* **2007,** *1* (Copyright (C) 2011 American Chemical Society (ACS). All Rights Reserved.), 63-69.
23. Zelikin, A. N.; Li, Q.; Caruso, F., Disulfide-Stabilized Poly(methacrylic acid) Capsules: Formation, Cross-Linking, and Degradation Behavior. *Chem. Mater.* **2008,** *20* (Copyright (C) 2011 American Chemical Society (ACS). All Rights Reserved.), 2655-2661.
24. Kozlovskaya, V.; Kharlampieva, E.; Erel, I.; Sukhishvili, S. A., Multilayer-derived, ultrathin, stimuli-responsive hydrogels. *Soft Matter* **2009,** *5* (Copyright (C) 2011 American Chemical Society (ACS). All Rights Reserved.), 4077-4087.
25. Kinnane, C. R.; Such, G. K.; Antequera-Garcia, G.; Yan, Y.; Dodds, S. J.; Liz-Marzan, L. M.; Caruso, F., Low-Fouling Poly(N-vinyl pyrrolidone) Capsules with Engineered Degradable Properties. *Biomacromolecules* **2009,** *10* (Copyright (C) 2011 American Chemical Society (ACS). All Rights Reserved.), 2839-2846.

26. De Koker, S.; De Geest, B. G.; Cuvelier, C.; Ferdinande, L.; Deckers, W.; Hennink, W. E.; De Smedt, S. C.; Mertens, N., In vivo Cellular Uptake, Degradation, and Biocompatibility of Polyelectrolyte Microcapsules. *Advanced Functional Materials* **2007,** *17* (18), 3754-3763.
27. Stadler, B.; Chandrawati, R.; Price, A. D.; Chong, S. F.; Breheney, K.; Postma, A.; Connal, L. A.; Zelikin, A. N.; Caruso, F., A microreactor with thousands of subcompartments: enzyme-loaded liposomes within polymer capsules. *Angew Chem Int Ed Engl* **2009,** *48* (24), 4359-62.
28. Bieber, T.; Meissner, W.; Kostin, S.; Niemann, A.; Elsasser, H. P., Intracellular route and transcriptional competence of polyethylenimine-DNA complexes. *J Control Release* **2002,** *82* (2-3), 441-54.
29. Godbey, W. T.; Wu, K. K.; Mikos, A. G., Size matters: molecular weight affects the efficiency of poly(ethylenimine) as a gene delivery vehicle. *J Biomed Mater Res* **1999,** *45* (3), 268-75.
30. Germain, M.; Balaguer, P.; Nicolas, J.-C.; Lopez, F.; Esteve, J.-P.; Sukhorukov, G. B.; Winterhalter, M.; Richard-Foy, H.; Fournier, D., Protection of mammalian cell used in biosensors by coating with a polyelectrolyte shell. *Biosensors and Bioelectronics* **2006,** *21* (8), 1566-1573.
31. Kozlovskaya, V.; Harbaugh, S.; Drachuk, I.; Shchepelina, O.; Kelley-Loughnane, N.; Stone, M.; Tsukruk, V. V., Hydrogen-bonded LbL shells for living cell surface engineering. *Soft Matter* **2011**.
32. Kharlampieva, E.; Kozlovskaya, V.; Sukhishvili, S. A., Layer-by-Layer Hydrogen-Bonded Polymer Films: From Fundamentals to Applications. *Advanced Materials* **2009,** *21* (30), 3053-3065.
33. Kozlovskaya, V.; Kharlampieva, E.; Drachuk, I.; Cheng, D.; Tsukruk, V. V., Responsive microcapsule reactors based on hydrogen-bonded tannic acid layer-by-layer assemblies. *Soft Matter* **2010,** *6* (15), 3596-3608.
34. Such, G. K.; Johnston, A. P. R.; Caruso, F., Engineered hydrogen-bonded polymer multilayers: from assembly to biomedical applications. *Chemical Society Reviews* **2011,** *40* (1), 19-29.
35. Erel-Unal, I.; Sukhishvili, S. A., Hydrogen-Bonded Multilayers of a Neutral Polymer and a Polyphenol. *Macromolecules* **2008,** *41* (11), 3962-3970.
36. Hushpulian, D. M.; Fechina, V. A.; Kazakov, S. V.; Sakharov, I. Y.; Gazaryan, I. G., Non-enzymatic interaction of reaction products and substrates in peroxidase catalysis. *Biochemistry (Mosc)* **2003,** *68* (9), 1006-11.
37. Takebayashi, J.; Tai, A.; Yamamoto, I., pH-dependent long-term radical scavenging activity of AA-2G and 6-Octa-AA-2G against 2,2'-azinobis(3-ethylbenzothiazoline-6-sulfonic acid) radical cation. *Biol Pharm Bull* **2003,** *26* (9), 1368-70.
38. Shutova, T.; Agabekov, V.; Lvov, Y., Reaction of radical cations with multilayers of tannic acid and polyelectrolytes. *Russian Journal of General Chemistry* **2007,** *77* (9), 1494-1501.
39. Kozlovskaya, V.; Yakovlev, S.; Libera, M.; Sukhishvili, S. A., Surface Priming and the Self-Assembly of Hydrogen-Bonded Multilayer Capsules and Films. *Macromolecules* **2005,** *38* (11), 4828-4836.

40. Koper, G. J. M.; van Duijvenbode, R. C.; Stam, D. D. P. W.; Steuerle, U.; Borkovec, M., Synthesis and Protonation Behavior of Comblike Poly(ethyleneimine). *Macromolecules* **2003,** *36* (7), 2500-2507.
41. Mészáros, R.; Thompson, L.; Bos, M.; de Groot, P., Adsorption and Electrokinetic Properties of Polyethylenimine on Silica Surfaces. *Langmuir* **2002,** *18* (16), 6164-6169.
42. Brunot, C.; Ponsonnet, L.; Lagneau, C.; Farge, P.; Picart, C.; Grosgogeat, B., Cytotoxicity of polyethyleneimine (PEI), precursor base layer of polyelectrolyte multilayer films. *Biomaterials* **2007,** *28* (4), 632-40.
43. Tsukruk, V. V.; Reneker, D. H., Scanning probe microscopy of organic and polymeric films: from self-assembled monolayers to composite multilayers. *Polymer* **1995,** *36* (9), 1791-1808.
44. Glinel, K.; Sukhorukov, G. B.; Möhwald, H.; Khrenov, V.; Tauer, K., Thermosensitive Hollow Capsules Based on Thermoresponsive Polyelectrolytes. *Macromolecular Chemistry and Physics* **2003,** *204* (14), 1784-1790.
45. Contributers, W. Fluorescence recovery after photobleaching. http://en.wikipedia.org/w/index.php?title=Fluorescence_recovery_after_photobleaching&oldid=406389463 (accessed 28 February).
46. Ibarz, G.; Dähne, L.; Donath, E.; Möhwald, H., Controlled Permeability of Polyelectrolyte Capsules via Defined Annealing. *Chemistry of Materials* **2002,** *14* (10), 4059-4062.
47. Glinel, K.; Dubois, M.; Verbavatz, J. M.; Sukhorukov, G. B.; Zemb, T., Determination of pore size of catanionic icosahedral aggregates. *Langmuir* **2004,** *20* (20), 8546-51.
48. Antipov, A. A.; Sukhorukov, G. B.; Donath, E.; Möhwald, H., Sustained Release Properties of Polyelectrolyte Multilayer Capsules. *The Journal of Physical Chemistry B* **2001,** *105* (12), 2281-2284.
49. Shutava, T. G.; Balkundi, S. S.; Vangala, P.; Steffan, J. J.; Bigelow, R. L.; Cardelli, J. A.; O'Neal, D. P.; Lvov, Y. M., Layer-by-Layer-Coated Gelatin Nanoparticles as a Vehicle for Delivery of Natural Polyphenols. *ACS Nano* **2009**.
50. Riedl, K. M.; Hagerman, A. E., Tannin-protein complexes as radical scavengers and radical sinks. *J Agric Food Chem* **2001,** *49* (10), 4917-23.
51. Lopes, G. K.; Schulman, H. M.; Hermes-Lima, M., Polyphenol tannic acid inhibits hydroxyl radical formation from Fenton reaction by complexing ferrous ions. *Biochim Biophys Acta* **1999,** *1472* (1-2), 142-52.
52. Sherman, F., Getting started with yeast. *Methods Enzymol* **2002,** *350*, 3-41.